Polytechnic of Turin

Master's Degree in Biomedical Engineering A.a 2022/2023

Graduate session October 2023

Computational investigation of tubulin mutations effect on colchicine binding site

Supervisors

Prof. Jacek TUSZYNSKI
Marco CANNARIATO

Candidate

Lorenzo BUFFONI

Acknowledgment

I am thankful to my supervisor professor Jack Tuszynski, whose unwavering support, invaluable expertise, and continuous encouragement were pivotal in shaping the direction and quality of this research.

I extend my appreciation to my family for their unending love, for always being there for me, for raising me the better they could and giving me the opportunity to live a happy and fulfilling life. In particular my mum Boss, my father Ba and my brother Faffy.

I would also like to thank all my friends for their encouragement, belief in my abilities and Gloria for sharing with me one of the best years of my life.

Lastly, I would like to remember all those who, like Madame Sir, support every day the fight to achieve more rights for all the women. They’re fight is our fight and for that, I am truly thankful.

Abstract

Colchicine derivatives are currently under scrutiny as potential candidates for future cancer therapeutic applications, leveraging the well-established antimitotic properties of colchicine. In this study, a comprehensive computational model of the colchicine binding site has been constructed within tubulin heterodimers. To achieve this, AlphaFold2 has been employed to generate three-dimensional structures of human beta tubulin in its wildtype and mutated form. A human alpha tubulin structure from available data bank online has been used to create the heterodimer, subsequently modifying the geometry of the heterodimer incorporating colchicine. This homology modeling approach was guided by crystallographic data from colchicine-docked microtubules in bovine cells.

This computational model was developed for various forms of the heterodimer, with a particular focus on different isotypes of beta tubulin that are known to be overexpressed in cancer tissues. To validate the model's accuracy and reliability, a rigorous comparison with experimental data derived from animal studies has been conducted.

Furthermore, the computational models were harnessed to perform docking simulations with colchicine, focusing on the variations in binding affinity induced by specific mutations within the colchicine binding site. This comprehensive analysis provides critical insights into the impact of distinct beta tubulin mutations on the colchicine binding site and offers valuable information essential for the design and development of highly targeted colchicine-based drugs tailored to tubulins overexpressed in cancer tissues. These findings represent a promising step towards the creation of more effective and specific cancer therapeutics.

Table of Contents

ACKNOWLEDGMENT **2**

ABSTRACT **3**

1. INTRODUCTION **8**

1.1. Cancer and antimitotic drugs 9
1.2. Colchicine 13
1.3. Colchicine devatives as a solution to colchicine's limitations 16

2 MATERIALS AND METHODS **17**

2.1.1. Human alpha tubulin isotype 17
2.2.2. Human beta tubulin isotypes 18
2.2.3. Research of the beta tubulin's residues involved in the colchicine binding site. 21
2.2.4. Use of Alphafold2 22
2.3.1. Quality assessment 23
2.3.2. Comparison of Alphafold2's human beta tubulin isotypes and human beta tubulin from cristallography 25
2.3.3. Comparison of human beta tubulin isotypes from Alphafold2 with animal tissue's beta tubulin 28
2.3.4. Binding site structure through MOE 30
2.4. Docking colchicine to colchicine binding site 33

RESULTS **37**

3.1.1. Docking of Colchicine in wild type tubulins 37
3.1.2. Docking of Colchicine in mutated tubulins 41

DISCUSSION **51**

CONCLUSION **55**

SUPPLEMENTARY INFORMATION **57**

LIST OF FIGURES **58**

LIST OF TABLES **60**

REFERENCES **62**

1. Introduction

In this study, an innovative in silico approach to investigate the impact of various mutations on the colchicine binding site has been employed. The methodology comprised the following steps:

1. Generation of Tubulin Heterodimer 3D Structure: starting by obtaining a high-quality 3D structure of the tubulin heterodimer using cutting-edge homology modeling techniques. Homology modeling, also known as comparative modeling, is a computational technique used in structural biology to predict the three-dimensional (3D) structure of a protein or other biomolecule based on the known structure of a related molecule. It relies on the principle that if two proteins share a high degree of sequence similarity (homology), they are likely to have similar 3D structures and perform similar functions.

   Specifically, AlphaFold2 has been leveraged, a state-of-the-art computational tool, to generate this structural model.

   AlphaFold2 starts with the protein's amino acid sequence and uses evolutionary data to guide predictions. Deep neural networks process this data to predict distances between amino acids in 3D space. An optimization process transforms these predictions into a 3D structure. The model's accuracy is assessed, and the final 3D protein structure is generated, aiding scientific research in various fields, including drug discovery and disease understanding.[1]

2. Defining the Binding Site Geometry: To precisely define the geometry of the colchicine binding site within the tubulin heterodimer, we employed Molecular Operating Environment (MOE). This step was instrumental in creating an accurate representation of the binding pocket.

3. Docking Simulations: A docking simulation is a computational technique used in molecular modeling to predict how two molecules, such as a protein and a small molecule drug, will interact and bind to each other. It

calculates the energetically favorable positions and orientations of the molecules relative to each other, providing insights into their potential binding affinity and mode of interaction. This information is valuable in drug discovery, as it helps researchers identify and design molecules that can effectively bind to a target protein, which is crucial for developing new medications. With the binding site geometry in place, we conducted docking simulations using both wild-type and mutated tubulins. These simulations allowed us to assess how colchicine binds to these protein variants and provided valuable insights into the affinity and strength of their interactions.

Through docking the goal is to predict the bound conformations (binding pose), using MOE's search algorithm, and the binding energy (affinity) of the investigated ligand for a specific receptor.

This comprehensive in silico approach offers a robust framework for unraveling the nuanced effects of different mutations on the colchicine binding site, shedding light on critical aspects of molecular interactions that are integral to our research endeavors.

1.1. Cancer and antimitotic drugs

The WHO (world health organization) data shows that cancer is the second leading cause of death globally and is responsible for 10 million deaths in a year worldwide (the number is increasing as years pass by). Globally, about 1 in 6 deaths is due to cancer[1].

Cancer is a complex disease characterized by the development of abnormal and malignant tumors, where cells multiply uncontrollably even when faced with limited resources and space. The growth of cancer cells is facilitated by the upregulation of telomerase expression, which counteracts telomere shortening and allows for unlimited replication potential. Furthermore, cancer cells possess the capability to evade tumor suppressor genes, leading to persistent and prolonged proliferation.[2]

[1] https://www.who.int

Currently, cancer treatment comprises a diverse range of options and protocols that are tailored to address the unique characteristics of each cancer type. This approach recognizes the individuality of cancer and acknowledges that different tumors necessitate specific treatments in order to maximize therapeutic efficacy.

One of the current treatments are antimitotic drugs.

Antimitotic drugs play a crucial role in inhibiting the polymerization dynamics of microtubules, specifically drugs like paclitaxel and vinblastine. By activating the spindle assembly checkpoint (SAC), these drugs effectively block the transition from metaphase to anaphase. Consequently, cells experience mitotic arrest. Due to the disruption of spindle formation and chromosome orientation caused by these compounds, cells either remain in a state of prolonged arrest, leading to apoptosis induction, or enter a senescence-like G1 state.

Antimitotic drugs that target microtubules have two distinct mechanisms of action:

microtubule-destabilizing agents and microtubule-stabilizing agents. Destabilizing drugs (Microtubule destabilizing agents MDA): hinder microtubule polymerization at high concentrations, with different types binding to specific domains, such as the vinca or colchicine domain. Examples of destabilizing drugs include vinflunine, vincristine, vinorelbine, vindesine, and eribulin, among others (Vinblastine and Vincristine for Vinca site).[3]

On the other hand, stabilizing drugs, when administered at high concentrations, enhance microtubule polymerization, stabilize microtubules (Microtubule stabilizing agents MSA), and prevent depolymerization triggered by factors like calcium or cold temperatures. Drugs in this category include eribulin, spongistatin, rhizoxin, taxanes (both second and third-generation), epothilones, ixabepilone, and several others (drugs like Paclitaxel, Docetaxel, Abraxan, Epothilone A and B for the taxane site) .[4]

These compounds bind to the inner surface of microtubules at specific taxoid-binding sites on β-tubulin.[5]

It’s possible to observe the mechanism of action of MSA and MDA in Figure 1

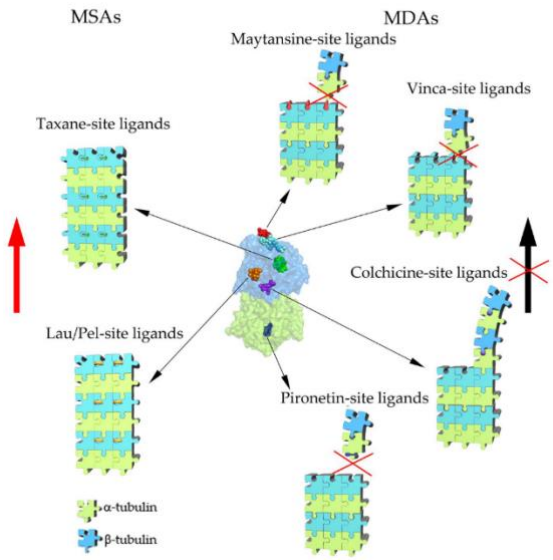

Figure 1- mechanism of action of stabilizer and destabiliser agents on MTs [6]

Drug resistance to anti-tubulin medications poses a significant clinical challenge in many chemotherapy treatments, and finding a definitive solution is complex.

Numerous research studies have shed light on the potential involvement of specific tubulin isotypes in the development of drug resistance. As our understanding grows, it becomes increasingly clear that isotype expression may contribute to drug resistance to some degree. Notably, the overexpression of βIII-tubulin has been identified as a key factor in antimitotic drugs resistance. This resistance mechanism reduces the stability of microtubules, thereby counteracting the efficacy of antimitotic drugs [6].

In Table 1 the main types of beta tubulin alterations are shown, the consequences caused by them, and the tumor associated with them.

Table 1: Principal Alteration of tubulin isotype [7]

Alteration of Tubulin Isotype	Effect	Tumour Type
High βI-tubulin	Poor response to docetaxel treatment	Breast cancer
Low βII-tubulin expression	Correlates with poor response to taxane treatment or advanced stage disease	Breast and ovarian cancer
High βIII-tubulin expression	Poor survival, poor outcome for surgical resection or TBA response; Correlates with subtype	Non-small cell lung cancer (NSCLC)
	Correlates with poor survival, poor response to platinum and taxane treatment, advanced stage or aggressive disease	Ovarian cancer
	Favourable response to taxane treatment	Ovarian (Clear cell adenocarcinoma)
	Poor response to taxane treatment	Breast cancer
	Poor response to taxane/platinum treatment	Uterine serous carcinoma
	Poor response to taxane treatment	Gastric cancer
	Advanced disease and early recurrence	Prostate cancer
High βIVa-tubulin expression	Poor response to taxol treatment	Ovarian cancer
High βV-tubulin expression	Favourable response to taxane treatment	NSCLC

Furthermore, certain microtubule-stabilizing drugs like peloruside A (PLA) and laulimalide bind to an overlapping non-vinca and non-taxoid site on drug-resistant βII- and βIII-tubulin isotypes. This binding results in a mitotic arrest at the G2/M phase of the cell cycle and eventual cell death. Notably, these compounds exhibit an advantage over taxanes and vinca alkaloids as they are less susceptible to P-gp drug efflux pumps, making them more effective in combating drug resistance.

During interphase, microtubules form and serve as vital components for accurate chromosome segregation and cell division during mitosis. Microtubule dynamics are notably faster during mitosis compared to interphase, making them an ideal target for drug intervention, particularly in cancer cells that exhibit hyperproliferative activity.[7]

Microtubules (MTs), as mentioned earlier, are essential components composed of numerous protein constituents. These proteins assemble, forming hollow tubes. These intricate structures are constructed through repetitions of a heterodimer, a combination of two globular proteins weighing 55 kDa each, known as α and β tubulin. The formation of the tubulin dimer occurs through a permanent binding process, where the individual α/β monomers unite, encapsulating a single molecule of GTP within the unchangeable nucleotide binding site of α tubulin.

The arrangement of α and β dimers within MTs follows a specific order, with a head-tail configuration. In this arrangement, the α subunit of one dimer is in contact with the β subunit of the subsequent dimer. This distinctive pattern imparts polarity to the microtubules, designating the β subunit as positive and the α subunit as negative. Thus, the MTs exhibit a discernible polarity, providing structural and functional characteristics to these dynamic cellular components.[1]

1.2. Colchicine

Colchicine is the most widely studied anti-mitotic agent to understand the dynamics and function of microtubules[8].

The medicinal plant Gloriosa superba is known for its abundant biosynthesis of colchicine($C_{22}H_{25}NO_{6)}$ [9] [10] [fig34], a bioactive molecule commonly used in the treatment of gout. Apart from its effectiveness in gout treatment, colchicine also exhibits antimitotic activity, making it a promising candidate for cancer research [10].

However, colchicine shows high toxicity also on normal cells, including neutropenia, gastrointestinal upset, bone marrow damage and anemia. Colchicine is not specific for cancer overexpressed isotypes, like isotype βIII; the therapeutic value of colchicine against cancer is restrained by its low therapeutic index. [11] ,[12].

Studies are currently underway to develop effective and less toxic colchicine semisynthetic formulations, with a focus on targeted drug delivery strategies for multiple solid cancers [10].

Colchicine has a long history of therapeutic use for various conditions such as familial Mediterranean fever, Behçet's syndrome, and liver cirrhosis. The compound was isolated in the 19th century and has been used to treat gout since ancient times. In recent years, there has been a shift towards utilizing natural products in a more sophisticated manner. Modern chemists have utilized compounds isolated from plants, like colchicine, as a basis for generating novel

derivatives that exhibit lower toxicity and hold potential in combating drug-resistant diseases.

The mechanism of action of colchicine involves binding at the interface between the α and β subunits of tubulin within the heterodimer at the carboxy terminal. This binding leads to modifications in the secondary structure of the tubulin protein. Colchicine interacts with three proteins: tubulin, cytochrome P450 3A4 (CYP3A4), and P-glycoprotein. Notably, colchicine can cross the blood-brain barrier, as a higher percentage of tubulin is present in the human brain. By binding to tubulin, colchicine disrupts microtubule polymerization, resulting in the inhibition of mitotic spindle formation, suppression of cell division, and induction of apoptosis [13].

Colchicine's elimination primarily occurs through the kidneys and liver, which can pose a risk of colchicine poisoning in patients with kidney or liver failure [10].

Colchicine binds with high affinity to tubulin that can become copolymerized into microtubules. Colchicine binding to β-tubulin results in curved tubulin dimer and prevents it to adopt a straight structure (colchicine binds at a location where it prevents curved tubulin from adopting a straight structure, which inhibits assembly) , due to a steric clash between colchicine and α-tubulin, which inhibits microtubule assembly [12] [14].

The colchicine molecule Figure 2 is composed of three rings, a trimethoxy benzene ring, (ring A), a methoxy tropone ring (ring C), and a seven-membered ring (ring B) carrying an acetamido group at its C7 position which anchors the A and C ring.

The A ring, in conjunction with the C ring, is essential for high-affinity binding to tubulin. Substituting methyl groups on the A ring with bulky groups reduces the potency of colchicine. The C ring, particularly the tropone ring, is crucial for the colchicine-tubulin interaction. Some compounds derived from the C ring, such as lumicolchicines and isocolchicine, have reduced binding ability. The B ring, although not essential, modulates the kinetic properties of colchicine-tubulin binding. Substituents on the B ring at the C7 position can influence the binding affinity. Various analogs of colchicine have been studied to understand their binding parameters and activity against tubulin [15].

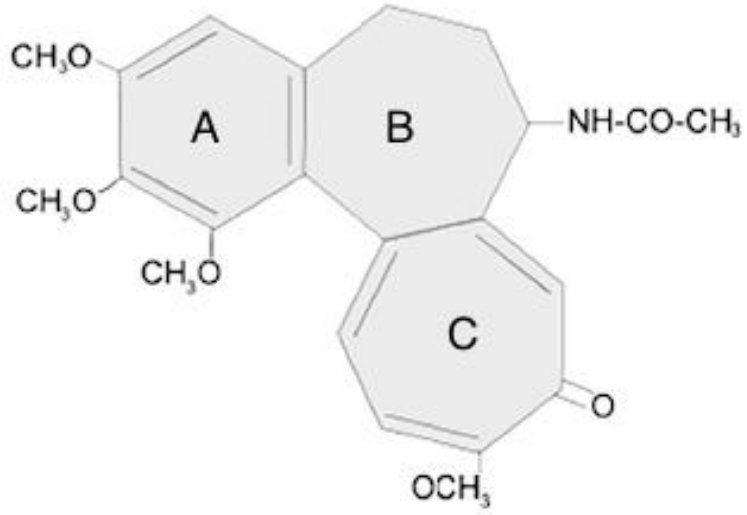

.

Figure 2: Colchicine's structure[9]

The size and substitution of groups on the A ring affect the potency of colchicine for tubulin binding. Modifications of the B-ring at the C7 position have led to active compounds with potential applications in cancer treatment. The C-ring, specifically the tropane ring, is crucial for colchicine-tubulin interaction. Modifications of the C-ring can result in changes in potency and selectivity against cancer cells. Various colchicine analogues with modified A, B, and C rings have been synthesized and evaluated for their anticancer activities. Some derivatives showed improved selectivity, reduced toxicity, and promising antitumor effects. These findings highlight the potential of colchicine derivatives as novel therapeutic agents for cancer treatment [13].

The colchicine binding site was identified by Ravelli et al. in 2004 by the determination of a 3.5 Å X-ray structure of α, β-tubulin complexed with N-deacetyl-N- (2-mercaptoacetyl) colchicine (DAMA-colchicine) [12].

Colchicine binds at the interface between the α and β subunits of tubulin within the heterodimer by H-bonding (with the Cys241 residue of β-tubulin) and hydrophobic interactions[13] (note: In many publications this residue is numbered as Cysβ239). The width of the colchicine binding site is approximately 4–5 Å, and the volume of this site is confined in β-tubulin by helix 7 (H7) containing Cysβ241, loop 7 (T7) and helix 8 (H8) [12].

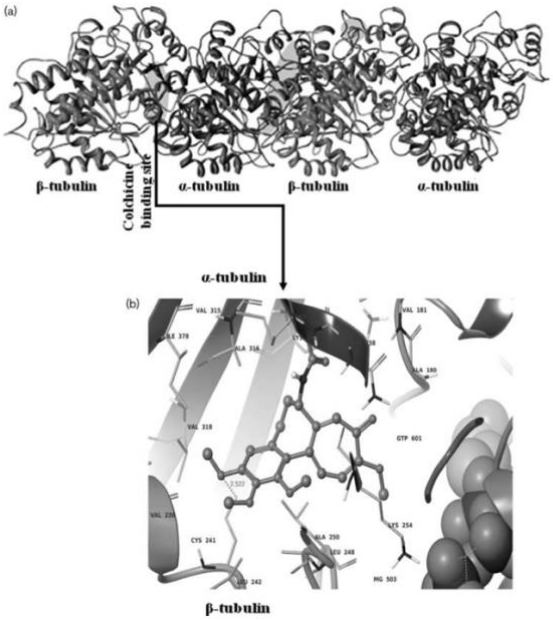

Figure 3: (a) Crystal structure of αβ-tubulin heterodimers showing the binding sites of colchicine. (b) Interactions of colchicine with the colchicine-binding site of tubulin.[13]

1.3. Colchicine devatives as a solution to colchicine's limitations

Novel Colchicine Derivatives have shown promise in downregulating the overexpression of P-glycoprotein genes, potentially overcoming multidrug resistance in cancer treatment [10].

these novel colchicine derivatives may be designed to show high specificity only for tubulin isotypes, which are over-expressed in cancer, in order to maximize their effect only on tumor cells and reduce side effects of the drug due to its toxicity on normal cells [11].

To develop better drug solutions using colchicine derivatives is fundamental to understand which is the influence of different cancer mutation of beta tubulin on colchicine's binding site.

In the following work will be modeled a colchicine binding site starting from human tubulin obtained through crystallography(alpha-tubulin), AlphaFold2 (beta-tubulin), an artificial intelligence (AI) program developed by DeepMind, a subsidiary of Alphabet, which performs prediction of protein structure, and the crystallography of the colchicine binding site, previously obtained from bovine tubulin.

In this study docking analyses were performed using a model of human tubulin heterodimers, both in their non-mutant form and with mutations found in tubulin overexpressed in cancerous tissue. The objective was to investigate the impact of these mutations on the binding site of colchicine. By employing colchicine in the docking simulations, we aimed to gain insights into how these genetic alterations may influence the interaction between tubulin and the drug.

2 Materials and methods

To understand the effects of tubulin mutations on the colchicine binding site, a model of the site has been created; the model consists in a human tubulin heterodimer composed by human alpha tubulin and a mutated version of human beta tubulin.

2.1.1. Human alpha tubulin isotype

In humans, the most common alpha tubulin isotype is known as alpha-1A/1B-tubulin (also referred to as TUBA1A or TUBA1B). This isotype is widely expressed in various tissues and cell types throughout the body. It forms the structural component of microtubules, which are essential for many cellular processes, including cell division, intracellular transport, and cell shape

maintenance. Alpha-1A/1B-tubulin is highly conserved across species and plays a crucial role in maintaining cellular structure and function [16]

This are the reasons why in this work has been used human Tubulin alpha-1B from the Protein Data Bank [17][2].

Figure 4: human Tubulin alpha-1B from the Protein Data Bank [17]

2.2.2. Human beta tubulin isotypes

In order to build mutated tubulins to dock with colchicine, a mutation database has been created [Table 1].

[2] https://www.rcsb.org/structure/6E7B

Table 2:the table has been made with mutations of β-Tubulin. Mutations A231T, L240I, F270V, T274I, R282N, Q292E, R306C, K350N of βIII tubulin are from [6]. All other mutations come from the Tubulin Mutation Database (TMD).

Beta	1		Beta	3		Beta	4	
T	33	S	T	166	A	E	45	D
T	35	N	V	170	M	N	48	S
V	60	F	S	172	A	V	64	I
L	112	P	V	180	A	A	124	C
I	152	T	I	189	V	S	126	N
I	155	V	A	218	T	A	154	C-b
P	171	L	A	231	T	I	155	V
D	177	G	S	239	C	V	189	I
T	237	H	L	240	I	T	218	A
T	238	H	D	249	E	C	239	R
C**	239	L	F	270	V	C	239	S
C**	239	Y	T	274	I	S	275	A
C**	239	P	A	275	S	Q	292	R
C**	239	R	A	275	T	A	315	T
L	240	P	R	282	N	N	332	A
R	241	P	Q	291	R	V	333	I
A	248	V	Q	292	E	N	335	S
A	248	T	M	293	V	T	351	V
L	273	P	K	297	R	A	365	S
K	324	R	R	306	C			
L	331	H	T	315	A			
T	351	V	R	320	P			
A	364	S	A	332	N			
V	365	S	I	333	V			
			S	335	N			
			K	350	N			
			V	351	T			
			A	352	V			
			S	364	A			
			S	365	A			
			S	365	V			
			I	374	T			
			T	386	S			

A database of mutated tubulin sequences has been built starting from information retrieved in previous literature and the Tubulin Mutation Database (TMD). Due to possible inconsistencies between literature and the TMD, tubulin β2 has not been considered in the analysis. The ensemble of mutations considered in this work is shown in Table 2. The mutated tubulin fasta sequences were automatically

built from Table 2. A MATLAB script, to obtain the mutated structure has been written.

Residues in *[*Table 2*]* signed with a -**- refers to residues that should be an 'S', but, in many papers/databases results as a 'C' [5], and in some uniport files as an E. This is a serious issue because the 239th residue is critical: according to [18] [19] it is a site of common interaction with small molecules, therefore, eventual mutations in that site may change the efficacy and/or the potency of many drugs. This residue is particularly important in the interaction with colchicine, due to the possible H-bonding interaction [12]**.**

In addition, the small molecule T007-1 was found to degrade tubulin isoforms that contain C239 (βII, βIV, and βV(β)), but not those that contain S239 (βIII, βVI), or mutant β-tubulin with a C239S substitution. Similarly, three other small molecules (T138067, EBI, and AITC) were also found to covalently bind to C239 of β-tubulin and induce degradation. These findings strongly suggest that the covalent modification of C239 by small molecules could be a novel strategy for promoting the degradation of tubulin heterodimers [19].

Table 3: table shows β III-tubulin mutations for different animal species and human β- tubulin mutations.

Novel mutations resembling βIII-tubulin in breast cancer

Table 1 Unique, conserved positions in βIII

βIII						Human					
Number	Human	Mouse	Chicken	*Xenopus*	Salmon	βI	βIIA	βIIB	βIVA	βIVB	βV
33	*S*	S	S	C	T	*T*	T	T	L	T	A
35	*N*	N	N	N	N	*T*	S	T	T	T	G
37	V	V	V	I	E	H	H	H	H	H	V
48	*S*	S	S	S	S	S	*N*	N	N	N	N
55	S	S	S	S	S	T	A	T	T	T	S
56	S	S	S	S	S	G	G	G	G	G	S
57	H	H	H	L	S	G	N	N	G	G	Q
80	A	A	A	A	T	P	P	P	P	P	P
83	H	H	H	H	Q	Q	Q	Q	Q	Q	Q
84	L	L	L	L	L	*I*	I	I	I	I	I
91	I	I	I	I	I	V	V	V	V	V	I
124	*C*	C	C	C	C	A	S	S	A	*A*	C
126	*N*	N	N	N	N	S	S	S	S	*S*	H
155	*V*	V	V	V	I	I	I	I	I	*I*	I
189	*I*	I	I	I	I	V	V	V	V	*V*	V
218	*A*	A	A	A	P	T	T	T	T	*T*	T
239	*S*	S	S	S	S	*C*	C	C	C	*C*	S
275	*A*	A	R	A	A	S	S	S	S	*S*	S
315	*T*	T	T	T	M	A	A	A	A	*A*	T
332	*A*	A	A	A	A	N	N	N	S	*N*	A
333	*I*	I	I	I	I	V	V	V	V	*V*	I
335	*S*	S	S	S	S	N	N	N	S	*N*	S
351	*V*	V	V	V	V	*T*	T	T	T	*T*	V
364	*S*	S	S	S	S	*A*	S	S	A	S	A
365	*S*	S	S	S	A	*V*	A	A	A	*A*	S

Positions and residues in italics indicate sites of mutations in breast cancer patients where βI, βIIA, or βIVB are mutated to positions corresponding to positions in βIII (also shown in italics). Note: the C-terminal amino acids (431-450) were not part of this study. Accession numbers: human βIII (AAL28094), mouse βIII (NP_075768), chicken βIII (NP_001026769), *Xenopus* βIII (NP_001088455), salmon βIII (XP_013982514), human βI (BAE78618), human βIIA (NP_001060), human βIIB (NP_821080), human βIVA (NP_001276058), human βIVB (NP_006079.1), and human βV (Q9BUF5)

As shown in *[Table 3]* [20] residue 239 is also critical in differentiation between the several types of β-tubulins. The figure also shows the relation between the mutations of the tubulin in different species.

2.2.3. Research of the beta tubulin's residues involved in the colchicine binding site.

The residues involved in the human colchicine binding site of tubulin primarily include amino acids from the β-tubulin subunit and alpha tubulin subunit. However, some commonly observed residues involved in the colchicine binding site of tubulin include: α Ala180, αVal181, βCys239, βLeu246, βAla248, βLeu253, βAla314 and βLys350.
These residues, among others, contribute to the interaction and binding of colchicine to the tubulin protein. It's worth noting that the binding site can also involve neighboring residues that contribute to the overall stability and specificity of the binding [21].

Comparing the residues involved in the colchicine binding site and the mutant residues from *[Table 2]*.

The following residues were selected has the mutant isotypes present in the colchicine binding site:

Table 4: the table shows mutations of β-Tubulin, present in the colchicine binding site

Beta	1		Beta	3		Beta	4	
C**	239	L				C	239	S
C**	239	Y				C	239	R
C**	239	P						
C**	239	R						
A	248	V						
A	248	T						
			K	350	N			

To obtain the 3D structure of this mutated versions has been used Alphafold2.

2.2.4. Use of Alphafold2

To obtain the 3D structure of the mutated proteins, Colabfold has been used[3], using the sequent parameters.

In this approach to using AlphaFold for protein structure prediction, several key decisions were made regarding its configuration and parameter settings.
Firstly, has been chosen to process one protein sequence at a time. While AlphaFold 1 allowed the processing of up to 20 sequences in a single run, we found this to be computationally inconvenient. Therefore, it has been opted for a more efficient approach, focusing on one sequence at a time to better manage computational resources.

Regarding energy relaxation during protein preparation in MOE, it has been set Num_relax to 0. This decision was made in anticipation of conducting energy relaxation as a separate step in the protein preparation process, likely using specialized software or methods tailored to this specific task.

When it came to shaping the protein structure, Template_mode = none has been selected. This choice was deliberate, as there wasn't the intention to impose a predefined shape onto the protein. Instead, the aim was to obtain initial results without any shape constraints, with the intention of validating these results in subsequent stages.

In terms of leveraging multiple sequence alignment (MSA) data for protein folding, Msa_mode = mmseqs2_uniref_env has been employed. This mode involved searching for similar sequences in the database (uniref_env) to enhance accuracy. This approach proved particularly valuable for proteins with low sequence identity to known structures.

---

3 https://colab.research.google.com/github/sokrypton/ColabFold/blob/main/AlphaFold2.ipynb

Regarding distance predictions, pair_mode = unpaired_paired has been utilized. This setting allowed AlphaFold to generate distance predictions for all residue pairs, irrespective of their contact status. This approach was beneficial for predicting the structures of highly disordered proteins. Alternatively, when set to "paired," AlphaFold focused solely on residue pairs predicted to be in contact. "Unpaired_paired" provided a dual approach, generating predictions for all residue pairs and paired residue pairs, thereby enhancing structural accuracy by utilizing both types of distance predictions.

For the multimeric model, the maximum number of recycles has been limited to 12. This decision resulted from careful experimentation, as increasing this parameter would have improved performance but at the cost of significantly higher computational resources. Our trials determined that a value of '12' struck an optimal balance.

Finally, the performance of all other parameters has been found to be satisfactory for the remainder of our research. Therefore, it has been chosen to retain their default 'auto' settings, as they met the requirements effectively [22]. These collective decisions in configuring AlphaFold2 allowed to tailor its functionality to the specific research needs, optimizing both accuracy and computational efficiency.

2.3.1. Quality assessment

In the quality assessment of a protein model the RMSD value and Z score provide important information:

1. RMSD (Root Mean Square Deviation): The RMSD measures the average discrepancy between the amino acid residues of the protein model and the corresponding residues of the reference structure. A lower RMSD value indicates a better structural alignment between the model and the reference structure. Typically, an RMSD value below 2 Å is considered good for high-quality protein models.

   RMSD is calculated by

$$\mathrm{RMSD} = \sqrt{\frac{1}{N}\sum_{i=1}^{N}\delta_i^2}$$

where δ is the distance between N pairs of equivalent atoms from the two coordinates[22,23]. This is often calculated for the backbone heavy atoms *C*, *N*, *O*, and C_α or sometimes just the C_α atoms. This value has been obtained through the dedicated option on MOE.

2. Z score: a Z-score, also known as a standard score, is a statistical measurement that quantifies the number of standard deviations a data point is from the mean (average) of a dataset. It is a way to standardize and compare data points from different distributions. The formula to calculate a Z-score for a data point (x) in a dataset with a mean (μ) and standard deviation (σ) is as follows:

$$Z = \frac{X - \mu}{\sigma}.$$

Where Z is the Z-score, x is the individual data point you want to standardize, μ id the mean (average) of the dataset and σ the standard deviation of the dataset.

The Z-score tells you how many standard deviations a data point is above or below the mean. A positive Z-score indicates that the data point is above the mean, while a negative Z-score indicates that it is below the mean. The magnitude of the Z-score indicates how far the data point is from the mean in terms of standard deviations.[22,23]

2.3.2. Comparison of Alphafold2's human beta tubulin isotypes and human beta tubulin from crystallography

To check the quality of the results given by AlphaFold2, the 3D structure of the tubulin β III has also been analyzed, and the results have been compared with the 3D structure of 5IJ0 model from RCSB protein data bank[24][4], this is also a human β III tubulin structure obtained through crystallography. The comparison hasn't been made for the β I and IV tubulins, because on the available protein banks are not present experimental structures, for these human isotypes.

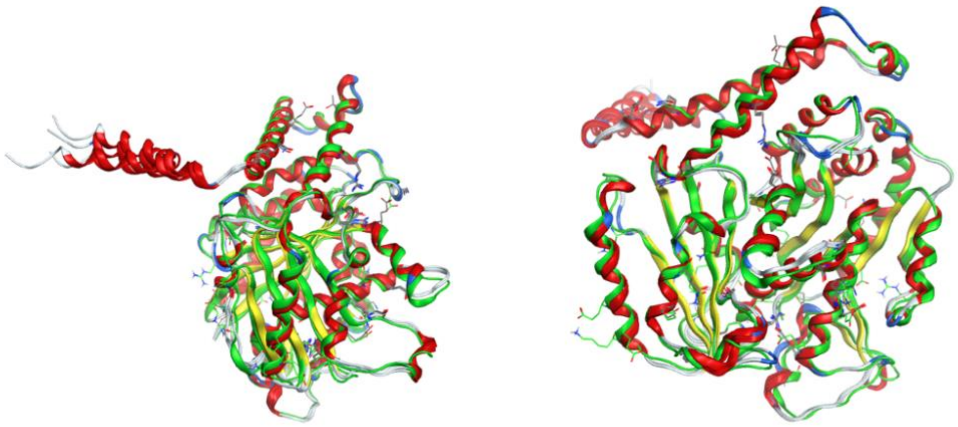

Figure 5: 3D representation of the 5 simulated models of the tubulin β III by Alphafold2 superposed with the ".pdb" human tubulin from RSCB in green, from two different points of view

[4] https://www.rcsb.org/structure/5IJ0

Table 5: Table of the average RMSD between the structures pictured in figure4, 5IJ0.B is the .pdb human tubulin from RSCB. The first five numbers are related to the five structures of human TUBB3 generated by Alphafold2.

RMSD = 0.706 A

	1	2	3	4	5	6
1: tub3_03...	0.00	0.51	0.36	0.53	0.31	0.96
2: tub3_03...	0.51	0.00	0.42	0.22	0.49	1.12
3: tub3_03...	0.36	0.42	0.00	0.44	0.29	1.08
4: tub3_03...	0.53	0.22	0.44	0.00	0.47	1.16
5: tub3_03...	0.31	0.49	0.29	0.47	0.00	1.04
6: 5IJ0.B	0.96	1.12	1.08	1.16	1.04	0.00

4.0 3.5 3.0 2.5 2.0 1.5 1.0 0.5 0.0

Alphafold2 gives 5 possible solutions to the input chain, so uploading all of them in MOE and superposing them as shown in Figure 5, the obtained RMSD is of about 1.07 Å average (as shown in Table 5), which is incredibly low given the differences in the predicted position of the side chain, clearly visible in Figure 5.

To give a metric of the quality of the protein model generated by Alphafold2, that could not be compared with human crystallography data, the Z score has been evaluated for the human TUBB1 not mutated and obtained with Alphafold2. The Z score of the protein is of -9.14 [Figure 6, Figure 7], which it is Z-scores comparable to experimental structures[25] and indicates the overall high quality of the model.

The value comes from a calculation made through Prosa online software[26][27][5].

[5] https://prosa.services.came.sbg.ac.at/prosa.php

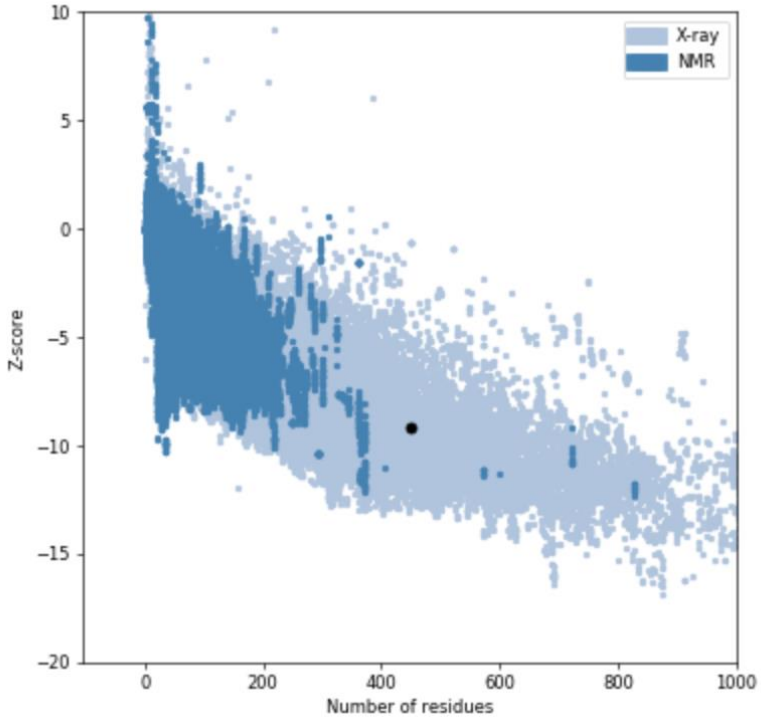

Figure 6: Z score value of wild-type human TUBB1 obtained with Alphafold2 is displayed in a plot. In this plot, structures from different sources (x-ray, NMR) are distinguished by different colours.

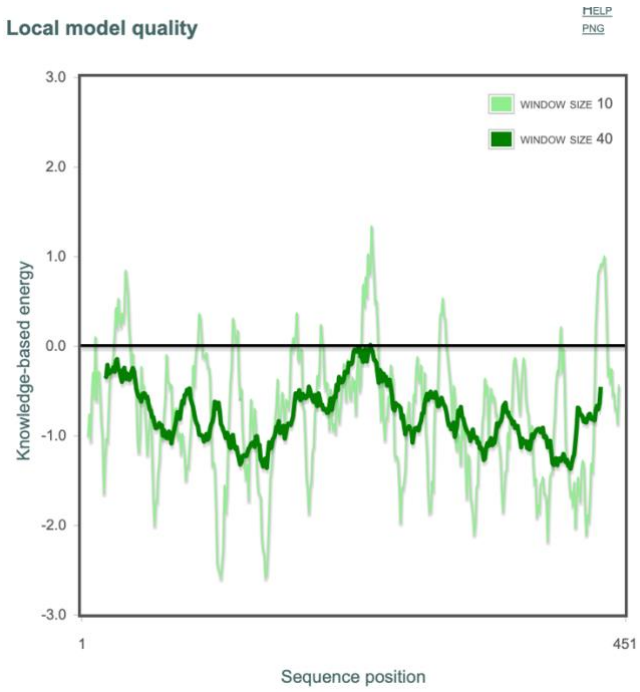

Figure 7: This plot shows local model quality by plotting energies as a function of amino acid sequence position i. In general, positive values correspond to problematic or erroneous parts of the input structure.

From Figure 7 a plot of single residue energies usually contains large fluctuations and is of limited value for model evaluation. Hence the plot is smoothed by

calculating the average energy over each 40-residue fragment *s(i,i+39)*, which is then assigned to the 'central' residue of the fragment at position *i+19* (thick line). A second line with a smaller window size of 10 residues is shown in the background of the plot (thin line).

Due to the high quality of the simulation that have been made to validate the efficacy of AlphaFold2's prediction, it has been possible to proceed simulating various 3D structures of the mutated primary sequence.

2.3.3. Comparison of human beta tubulin isotypes from Alphafold2 with animal tissue's beta tubulin

To further validate the results given by AlphaFold2, to endorse the use of animal tubulin heterodimer as a template and to understand how similar animal tubulin used in vitro analysis are to human tubulin (which are the actual target of drug therapy), the RMSD was calculated, between human beta tubulin structures obtained with Alphafold2 and animal tubulin structures from crystallography, in particular has been used beta tubulin from bovine tissue. This bovine tubulin is often chosen to study tubulin and his interaction with colchicine. The chosen bovine tubulin comes from the PDB[28][6]here is docked with colchicine Figure 8. Bovine tubulin and human tubulin are very similar in terms of their amino acid sequence (about 98-99% identical) and 3D structure, but it is a non-idealistic situation.

[6] https://www.rcsb.org/structure/4O2B

Figure 8: Bovine tubulin from RCSB [28] docked with colchicine.

All the results showed a RMSD value below 2 Å, indicating the high quality of the tubulin models.

The RMSD between the bovine tubulin and the mutated forms is of 0.571 Å Figure 9, the difference between the mutated forms is extremely low; more evident is the difference with the bovine tubulin (402B.B in Figure 9).

When you observe a peak in the RMSD value associated with a specific residue in a protein, it indicates that this particular residue is experiencing a significant conformational change or deviation between the two structures being compared.

In Figure 9 there aren't peaks which underlines the similarity between the bovine and human tubulin.

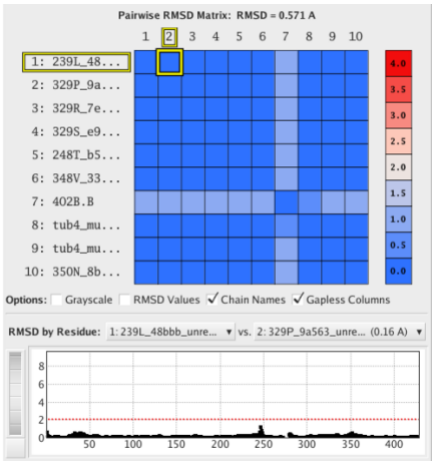

Figure 9: RMSD between bovine beta tubulin (402B.B) and human mutated beta tubulin obtained through Alphafold2. The RMSD value associated to specific residues doesn't present peaks.

The RMSD has between evaluated even between the wildtype isotypes obtained with Alphafold2 and the bovine tubulin [Figure 10].

The root-mean-square deviation (RMSD) between the wild-types of human tubulin TUBB1 and bovine tubulin is 0.788 Å. When comparing wild-type human TUBB3 to bovine tubulin, the RMSD value is 1.069 Å, and for wild-type human TUBB4 compared to bovine tubulin, the RMSD value is 1.113 Å.[29]

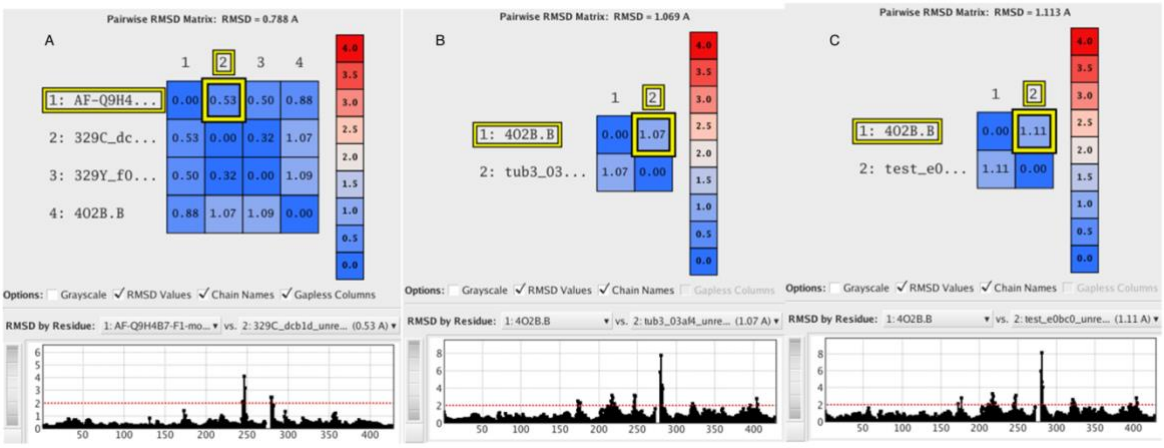

Figure 10: A) The RMSD of wild-type form of human tubulin TUBB1 E239, C239, Y239 and bovine tubulin (402B.B) is of 0.788 Å, B) between wild-type humanTUBB3 and bovine tubulin the value of RMSD is of 1.069 Å and C) the value of RMSD between wild-type human TUBB4 and bovine tubulin is of 1.113 Å. The RMSD shows some peak in correspondence on the residues that differ.

The peaks in the RMSD value associated with a specific residue are related to the different residues specific of each isotype. This local structural change It's an intrinsic characteristic of each isoform that doesn't significantly affect the final RMSD value.

2.3.4. Binding site structure through MOE

A colchicine binding site was constructed in MOE, utilizing a colchicine-tubulin complex obtained via X-ray diffraction [30][7] as a guiding template. The template comprises two tubulin heterodimers: Tubulin beta-2B chain (organism: Bos taurus) and Tubulin alpha-1B chain (organism: Bos taurus). Moreover, the template also encompasses the molecules found within microtubules:

ACP PHOSPHOMETHYLPHOSPHONIC ACID ADENYLATE ESTER, CA CALCIUM ION, GDP GUANOSINE-5'-DIPHOSPHATE, GOL GLYCEROL , GTP GUANOSINE-5'-TRIPHOSPHATE, IMD IMIDAZOLE, LOC N-[(7S)-1 ,2,3,10-tetramethoxy-9-oxo-6,7-dihydro-5H-benzo[d]heptalen-7-yl]ethanamide (colchicine), MES 2-(N-MORPHOLINO)-ETHANESULFONIC ACID, MG M AGNESIUM ION, PEG DI(HYDROXYETHYL)ETHER.

The complex employed for constructing various forms of the heterodimer comprises one heterodimer and includes GDP, LOC, GTP, and MG molecules. The molecules have been chosen, because of their role in influencing the colchicine binding site [31]**.**
These forms were built using different isotypes of beta tubulin, which were overexpressed in cancer tissues.
Every beta tubulin obtained with Alphafold2 have been aligned and superposed to the bovine alpha tubulin of the template, each time even the human alpha-tubulin has been added by alignment and superposing.
After superposing the alpha and beta structure to the template the following steps have been adopted to prepare the geometry of the colchicine binding site of the template for docking, maintaining the ligand's structure:

-hydrogen atoms (protons) were added to the 3D molecular structures. The addition of hydrogen atoms is important because it influences the overall charge distribution and can significantly affect the behavior and interactions of the molecules during simulations or calculations.

In order to achieve this, the "Protonate 3D" feature within MOE has been employed. When configuring this option, specific choices have been made to align with the requirements. The temperature has been set to 300 degrees, the pH to 7.4, and the salt concentration to 0.15. These parameter values were selected based on the understanding of physiological conditions and the relevant biological context. In essence, the settings have been tailored to mimic the physiological environment to ensure the accuracy and relevance of our results.

[7] https://www.rcsb.org/structure/4O2B

- energy minimization. This feature from MOE has been used to optimize the 3D geometry of the molecular structures by finding a local energy minimum in the potential energy surface of the system.

The goal of energy minimization is to achieve a stable and low-energy conformation of the molecule, representing its most energetically favorable arrangement under the given force field and molecular environment. This process is essential for preparing molecular structures for docking studies.

Prior to initiating the energy minimization process, various steps were taken to prepare the system. Initially, the molecules GDP, MG, LOC, and GTP were held in place, while the carbon atoms within the heterodimer were restricted, ensuring stability within the system.

Conversely, the procedure was then reversed. In this phase, the small molecules were tethered, and the heterodimer was firmly fixed to create a different configuration that would subsequently be subjected to energy minimization.

Following these initial preparations, the ligands were tethered, while the receptor was allowed to move freely. This step aimed to find an energetically favorable arrangement between the ligands and the unrestrained receptor before commencing the energy minimization.

Continuing the process, the ligands were released from their tethered positions, and the receptor was once again tethered. This allowed for the exploration of potential conformations and interactions as the system was readied for further minimization.

In the final stages, both the receptor and ligands were simultaneously released, marking the last phase of the minimization process. This comprehensive approach aimed to optimize the entire system's energy and achieve the most stable configuration.
The previous procedure was carried out in order to preserve the structure of the ligands while simultaneously enabling the heterodimer to accommodate the ligands within the binding site.
In MOE "fix" and "tether" are two options used to control the movement or behavior of specific atoms or groups within a molecular system; "fix" immobilizes selected atoms or groups, while "tether" allows controlled movement within a defined region.

The minimizing procedure has been successful.

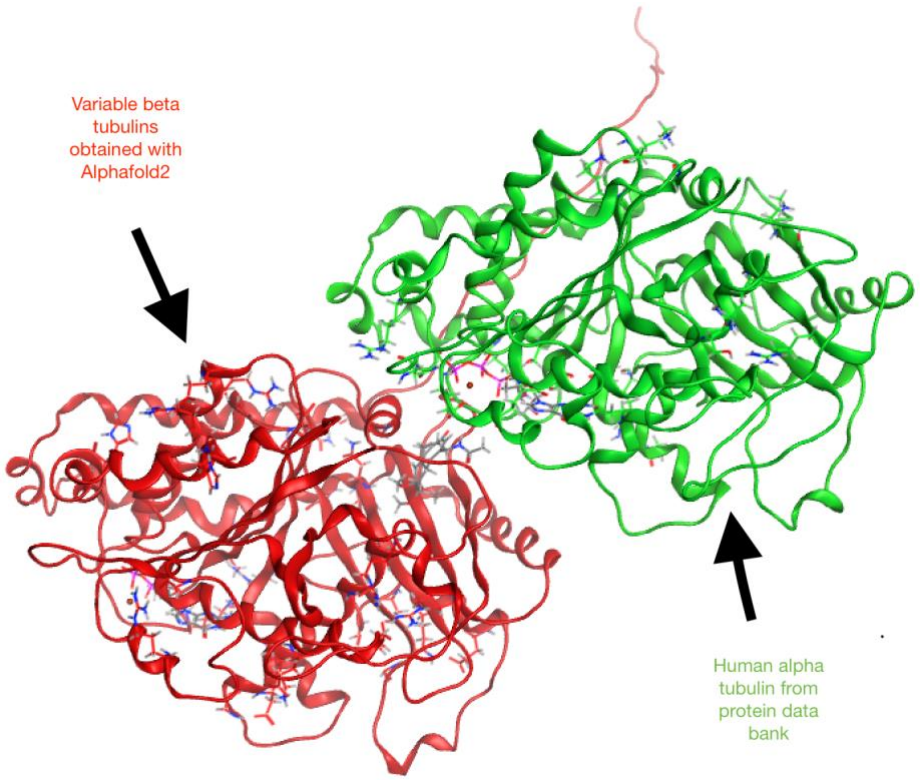

Figure 11: 3D structure of the obtained heterodimer composed by a beta tubulin structure from Alfafold2 and an alpha tubulin from RSCB.

At the end of this process the resultant heterodimers have the structure presented in Figure 11and are composed as shown below:

-Human alpha tubulin and not mutant beta 1 tubulin (TUBB1 Y239, C239, E239)
-Human alpha tubulin and not mutant beta 3 tubulin (TUBB3)
-Human alpha tubulin and not mutant beta 4 tubulin (TUBB4)

-Human alpha tubulin and mutant beta 1 (TUBB1 239L, 239P, 239R, 239S, 248T, 248V)
-Human alpha tubulin and mutant beta 3 (TUBB3 K350N)
-Human alpha tubulin and mutant beta 4 (TUBB4 C239R, C239S)

2.4. Docking colchicine to colchicine binding site

In the bovine tubulin used as template the interaction with colchicine has been investigated. Through the MOE, has been possible to automatically find the interested site and the amino acids directly involved in it, as reported in Figure 13. The type of interaction, the distance of the interaction and the energy involved are shown in Table 6.

Table 6: Table of the interactions between LOC and non-mutated crystallography bovine tubulin heterodimer.

Ligand	Receptor	Interaction	Distance	E (kcal/mol)
C18 29	SD MET 259 (B)	H-donor	3.71	-0.8
O1 15	ALA 316 (B)	H-acceptor	3.30	-0.6
O3 19	CB CYS 241 (B)	H-acceptor	3.56	-0.5
O5 27	CA ALA 180 (A)	H-acceptor	3.26	-1.0
O5 27	N VAL 181 (A)	H-acceptor	3.05	-3.0

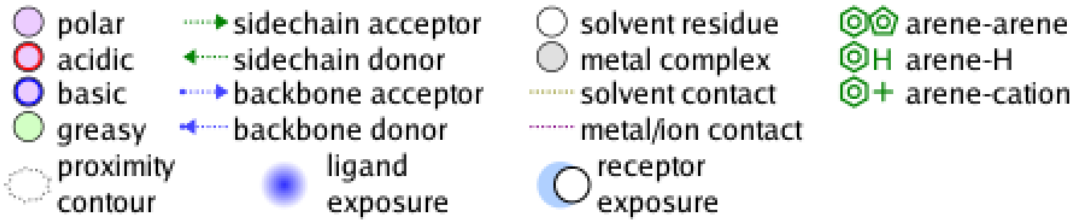

Figure 12:legend for all following interactions of the ligand with the receptor from MOE

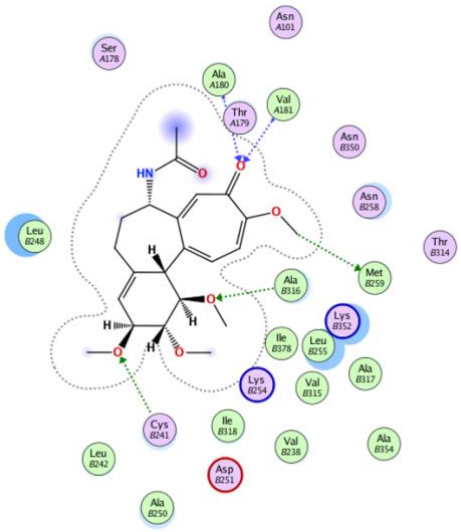

Figure 13:bovine tubulin heterodimer obtained through crystallography, in its interaction with colchicine.

In 2006 research, [32]an optimal energy would have been more than -8 kcal/mol.
On the other hand, many H-bond implies a reliable connection.

The docking between Colchicine (LOC) and the tubulin heterodimers has been performed using the following parameters:
Triangle matching as placement method.
This is a placement method used in molecular docking. It involves dividing the ligand molecule into triangles and matching these triangles with complementary regions on the protein's surface. The goal is to find a favorable initial position for the ligand within the binding site of the receptor.
100 placement poses.
These refer to the different initial positions or orientations of the ligand within the receptor's binding site that are generated during the placement phase of molecular docking. Multiple placement poses are often generated to explore potential binding modes of the ligand.
Rigid receptor as refinement method.
This is a refinement method used in molecular docking. In this method, the protein receptor is held fixed or rigid while the ligand is allowed to move and optimize its position and conformation. The rigid receptor approach assumes that the protein structure remains unchanged during the binding process.
1 refinement pose.
After the initial placement of the ligand and the rigid receptor refinement, the ligand's position and conformation are further optimized to achieve a more accurate binding pose. The refinement pose represents the final, energetically favorable orientation of the ligand within the binding site.

The docking has been performed between the two heterodimers and not only the colchicine, but all the molecules involved in the docking binding site (MG, GDP, GTP); even if the docking parameters analyzed, in the current work are the ones referring to Colchicine.

To evaluate the strength of the bond between the pocket and the molecule, the S score has been considered; it has been obtained with the performed docking procedure: a negative logarithmic value of the predicted dissociation constant (Kd) in units of Molarity (M). The lower the S score, the higher the predicted binding affinity between the protein and the ligand. Typically, S scores range from -15 to 0, with more negative values indicating better binding.[33] The S score is a scoring function, and like any scoring function, it possesses its own set of strengths and limitations. Therefore, in the context of this study, it should be regarded as a comparative measure of interaction affinity rather than being interpreted strictly for its physical significance.
The physical meaning of the S score is the energy difference between the bound and unbound states of the protein-ligand complex. In other words, the S score represents the free energy change upon binding of the ligand to the protein.
Free energy is described by the equation below:

$$\Delta G = \Delta G^o + RT \ln \kappa$$

In this context, "R" represents the universal gas constant, "T" denotes the temperature, and "K" stands for a constant. At equilibrium, when ΔG = 0, the reaction quotient (the term within the logarithm) equals the equilibrium constant. This relationship leads to the following:

$$\Delta G^o = -R\,T\ \ln K$$

K experimental values for colchicine to tubulin binding can be found in literature and delta G can be obtained from experimental values of K and this could be used to calibrate the S score[34].
A more negative S score indicates a stronger binding between the two molecules, which can be translated into a higher probability of the ligand being able to exert its biological activity.
Giving these docking parameters, the next step has been to attempt to dock the LOC firstly to the non-mutated human tubulin heterodimers and then to the mutated structures.

Results

3.1.1. Docking of Colchicine in wild type tubulins

TUBB1 C239 wild type.

The S score obtained through MOE for this interaction is of S= -8.98946328, the geometry of the interaction is shown in Figure 14 and the type of interaction with the associated distance and energy are represented in Table 7.

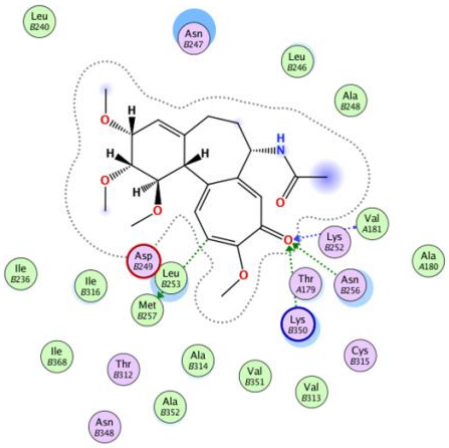

Figure 14: LOC docked to human βI-tubulin (TUBB1 C239)

Table 7: Table of the interactions between LOC and wild type human βI-tubulin (TUBB1 C239)

Ligand	Receptor	Interaction	Distance	E (kcal/mol)
C19 49	SD MET 257 (A)	H-donor	3.81	-0.6
O5 53	N VAL 181 (A)	H-acceptor	3.04	-0.9
O5 53	ND2 ASN 256 (A)	H-donor	2.75	-0.5
O5 53	CE LYS 350 (A)	H-acceptor	3.06	-0.5

TUBB1 E239 wild type.

The S score obtained through MOE for this interaction is of S= -9.11894321, the geometry of the interaction is shown in Figure 14 and the type of interaction with the associated distance and energy are represented in Table 8.

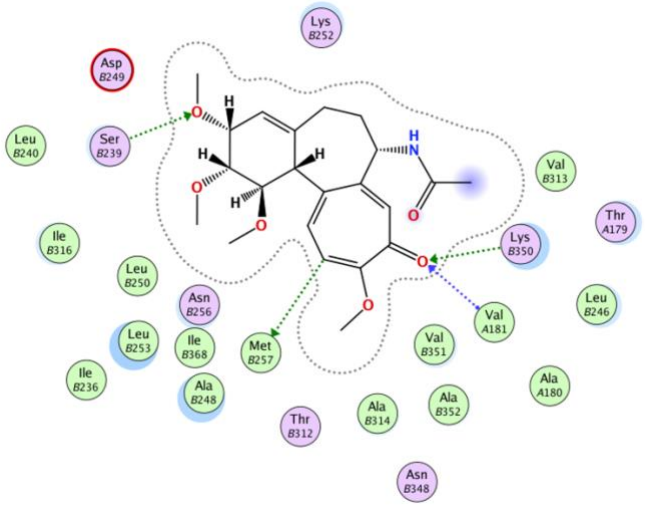

Figure 15:LOC docked to human βI-tubulin (TUBB1 E239)

Table 8: Table of the interactions between LOC and wild type human βI-tubulin (TUBB1 E239)

Ligand	Receptor	Interaction	Distance	E (kcal/mol)
C19 49	SD MET 257 (A)	H-donor	3.73	-0.6
O3 39	OG SER 239 (A)	H-acceptor	2.92	-1.4
O5 53	N VAL 181 (A)	H-acceptor	3.09	-2.5
O5 53	NZ LYS 350 (A)	H-acceptor	2.82	-0.5

TUBB1 Y239 wild type.

The S score obtained through MOE for this interaction is of S=-10.7720346, the geometry of the interaction is shown in Figure 16 and the type of interaction with the associated distance and energy are represented in Table 9.

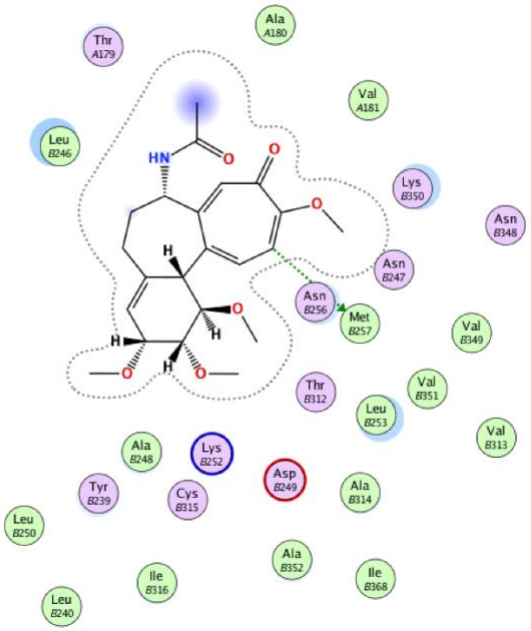

Figure 16:LOC docked to human βI-tubulin (TUBB1 Y239)

Table 9: Table of the interactions between LOC and wild type human βI-tubulin (TUBB1 Y239)

Ligand	Receptor	Interaction	Distance (A)	E (kcal/mol)
C19 49	SD MET 257 (A)	H-donor	3.85	-0.6

TUBB3 wild type.

The S score obtained through MOE for this interaction is of S=-8.97283519, the geometry of the interaction is shown in Figure 17 and the type of interaction with the associated distance and energy are represented in Table 9.

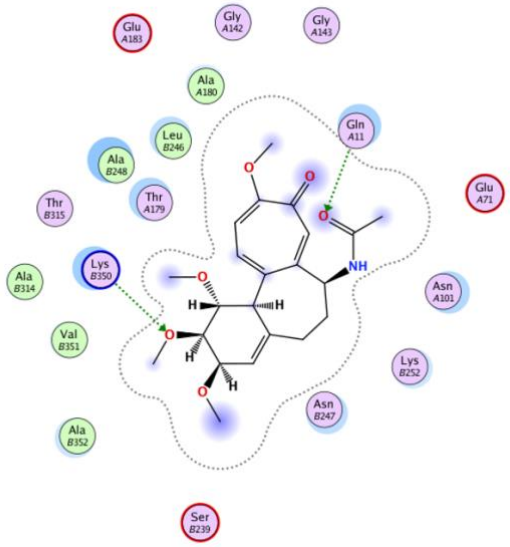

Figure 17:LOC docked to human βIII-tubulin (TUBB3)

Table 10: Table of the interactions between LOC and wild type human βIII-tubulin (TUBB3)

Ligand	Receptor	Interaction	Distance (A)	E (kcal/mol)
O4 1	1 NE2 GLN 11 (A)	H-acceptor	2.62	-2.1
O2 34	CE LYS 350 (A)	H-acceptor	3.01	-1.2

TUBB4 wild type.

The S score obtained through MOE for this interaction is of S= -9.44299793, the geometry of the interaction is shown in Figure 18 and the type of interaction with the associated distance and energy are represented in Table 11.

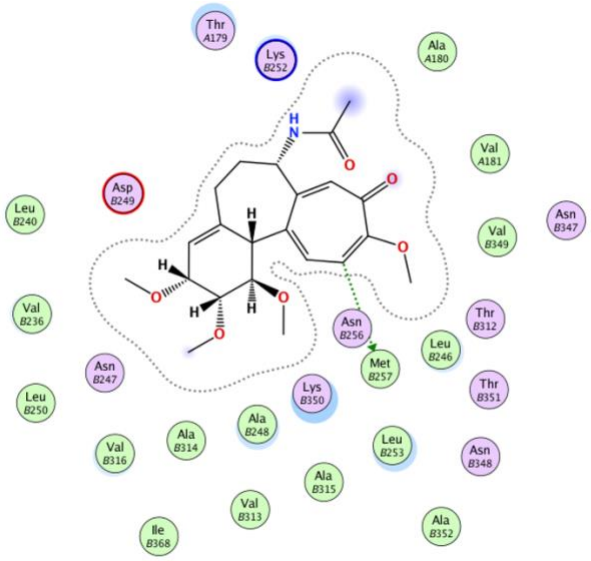

Figure 18:LOC docked to human βIV-tubulin (TUBB4)

Table 11:Table of the interactions between LOC and wild type human βIV-tubulin (TUBB4)

Ligand	Receptor	Interaction	Distance (A)	E (kcal/mol)
C19 49	SD MET 257 (A)	H-donor	3.87	-0.5

3.1.2. Docking of Colchicine in mutated tubulins

TUBB1 C239L

The S score obtained through MOE for this interaction is of S=-11.2332296, the geometry of the interaction is shown in Figure 19 and the type of interaction with the associated distance and energy are represented in Table 12.

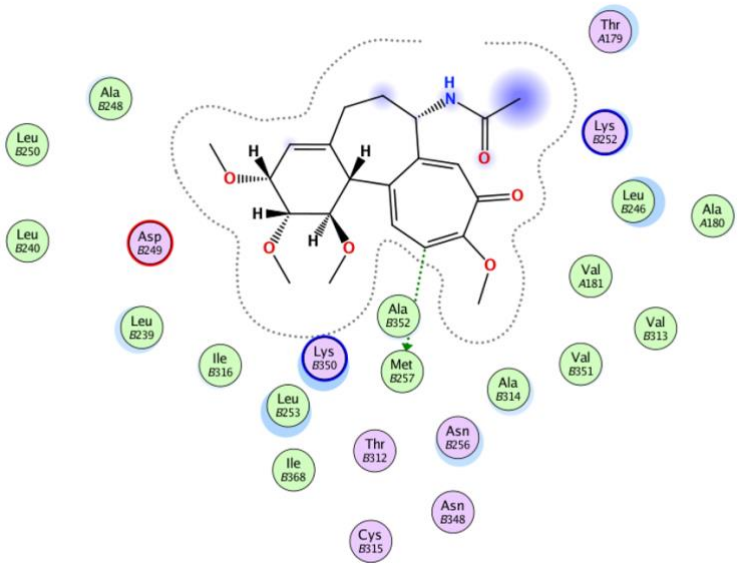

Figure 19: LOC docked to a mutated human βI-tubulin (TUBB1 C239L)

Table 12:Table of the interactions between LOC and mutated human βI-tubulin (TUBB1 C239L)

Ligand	Receptor	Interaction	Distance (A)	E (kcal/mol)
C19 49	SD MET 257 (A)	H-donor	3.98	-0.5

TUBB1 C239P

The S score obtained through MOE for this interaction is of S= -8.88401794, the geometry of the interaction is shown in Figure 20 and the type of interaction with the associated distance and energy are represented in Table 12.

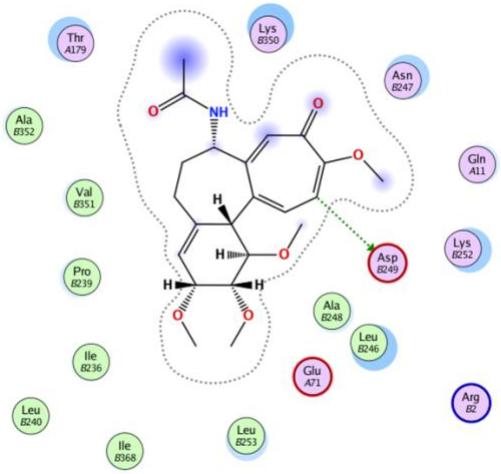

Figure 20:LOC docked to a mutated human βI-tubulin (TUBB1 C239P)

Table 13:Table of the interactions between LOC and mutated human βI-tubulin (TUBB1 C239P)

Ligand	Receptor	Interaction	Distance (A)	E (kcal/mol)
C19 49	OD2 ASP 249 (A)	H-donor	3.26	-1.0

TUBB1 C239R

The S score obtained through MOE for this interaction is of S= S=-10.9984837, the geometry of the interaction is shown in Figure 21 and the type of interaction with the associated distance and energy are represented in Table 14.

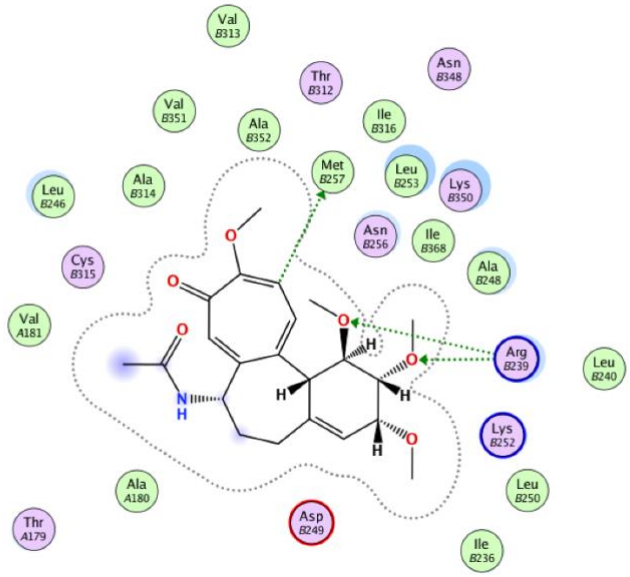

Figure 21: LOC docked to a mutated human ꞵI-tubulin (TUBB1 C239R)

Table 14:Table of the interactions between LOC and mutated human ꞵI-tubulin (TUBB1 C239R)

Ligand	Receptor	Interaction	Distance (A)	E (kcal/mol)
C19 49	SD MET 257 (A)	H-donor	3.85	-0.6
O1 29	NH2 ARG 239 (A)	H-acceptor	2.68	-4.2
O2 34	NE ARG 239 (A)	H-acceptor	2.75	-1.6
O2 34	NH2 ARG 239 (A)	H-acceptor	2.58	-1.4

TUBB1 C239S

The S score obtained through MOE for this interaction is of S=-9.09840298, the geometry of the interaction is shown in Figure 21 and the type of interaction with the associated distance and energy are represented in Table 15.

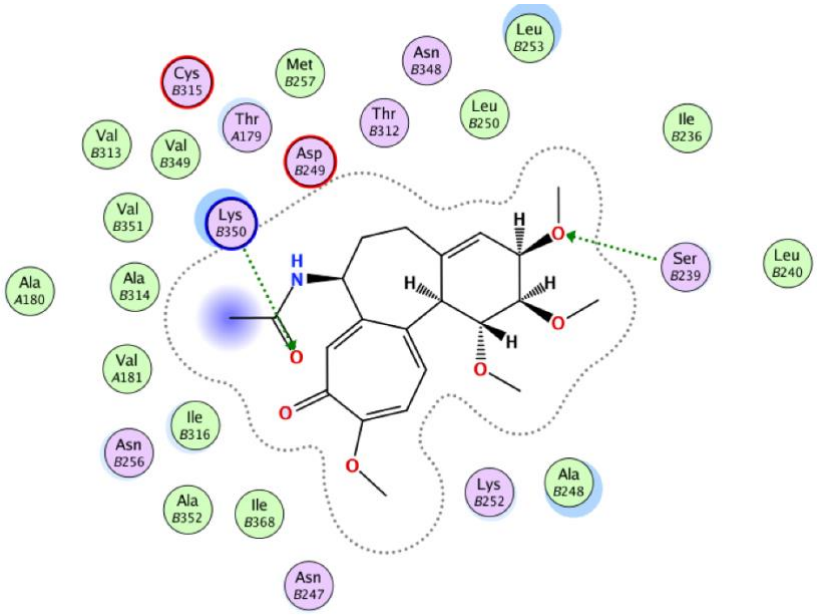

Figure 22:LOC docked to a mutated human βI-tubulin (TUBB1 C239S)

Table 15:Table of the interactions between LOC and mutated human βI-tubulin (TUBB1 C239S)

Ligand	Receptor	Interaction	Distance (A)	E (kcal/mol)
O4 1	NZ LYS 350 (A)	H-acceptor	2.80	-2.1
O3 39	OG SER 239 (A)	H-acceptor	3.09	-0.6

TUBB1 A248T

The S score obtained through MOE for this interaction is of S= -10.0235205, the geometry of the interaction is shown in Figure 23 and the type of interaction with the associated distance and energy are represented in Table 16.

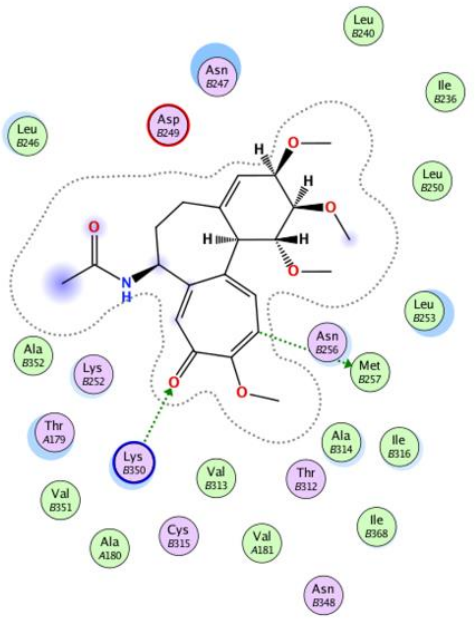

Figure 23:LOC docked to a mutated human βI-tubulin (TUBB1 C248T)

Table 16:Table of the interactions between LOC and mutated human βI-tubulin (TUBB1 C248T)

Ligand	Receptor	Interaction	Distance (A)	E (kcal/mol)
C19 49	SD MET 257 (A)	H-donor	4.10	-0.5
O5 53	NZ LYS 350 (A)	H-acceptor	2.81	-5.2

TUBB1 A248V

The S score obtained through MOE for this interaction is of S=-8.69873333, the geometry of the interaction is shown in Figure 23 and the type of interaction with the associated distance and energy are represented in Table 17.Table 17:Table of the interactions between LOC and mutated human βI-tubulin (TUBB1 C248V)

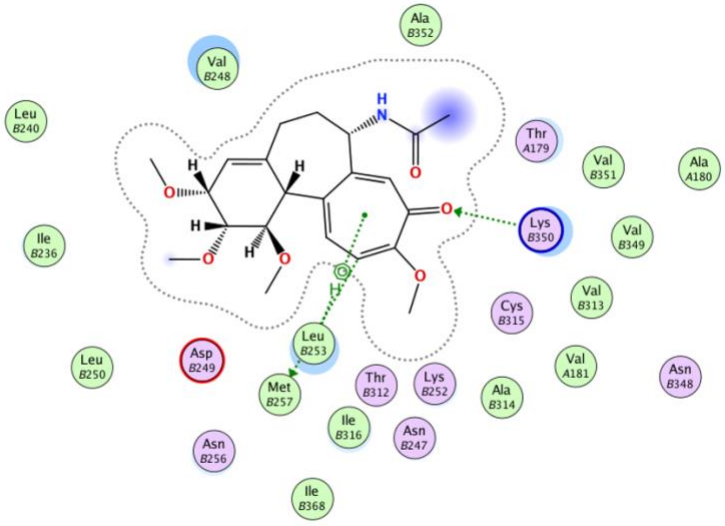

Figure 24:LOC docked to a mutated human βI-tubulin (TUBB1 C248V)

Table 17:Table of the interactions between LOC and mutated human βI-tubulin (TUBB1 C248V)

Ligand	Receptor	Interaction	Distance (A)	E (kcal/mol)
C19 49	SD MET 257 (A)	H-donor	4.04	-0.5
O5 53	C NZ LYS 350 (A)	H-acceptor	2.88	-4.3
7-ring	CA LEU 253 (A)	pi-H	5.05	-0.5

TUBB3 K350N

The S score obtained through MOE for this interaction is of S=-10.4061117, the geometry of the interaction is shown in Figure 23 and the type of interaction with the associated distance and energy are represented in Table 16.

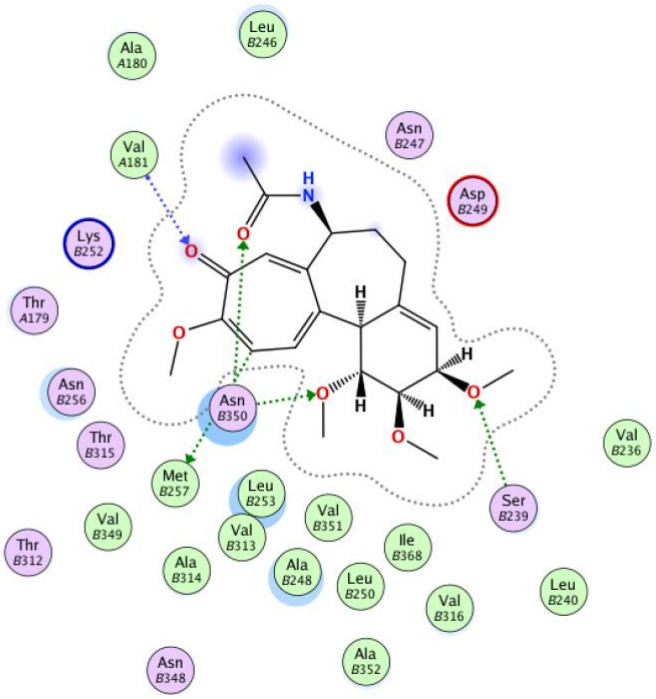

Figure 25: LOC docked to a mutated human βIII-tubulin (TUBB3 K350N)

Table 18: Table of the interactions between LOC and mutated human βIII-tubulin (TUBB3 K350N)

Ligand	Receptor	Interaction	Distance (A)	E (kcal/mol)
C19 49	SD MET 257 (A)	H-donor	3.99	-0.5
O4 1	ND2 ASN 350 (A	H-acceptor	3.07	-2.2
O1 29	29 ND2 ASN 350 (A)	H-acceptor	3.18	-0.5
O3 39	OG SER 239 (A)	H-acceptor	2.93	-1.3
O5 53	N VAL 181 (A)	H-acceptor	3.01	-2.6

TUBB4 C239R

The S score obtained through MOE for this interaction is of S=- 8. 95020164, the geometry of the interaction is shown in Figure 26 and the type of interaction with the associated distance and energy are represented in Table 19.

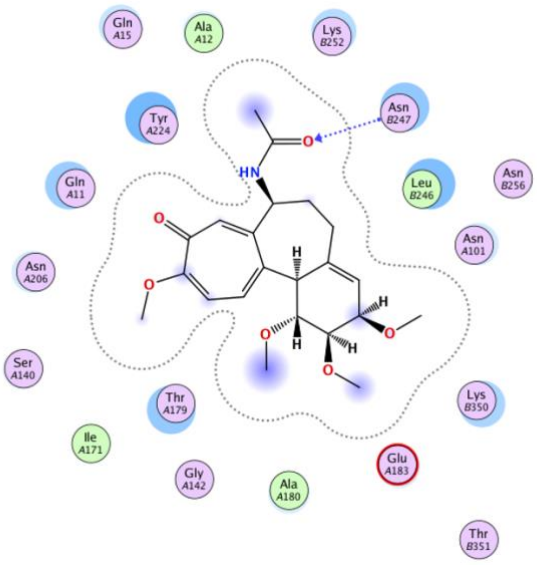

Figure 26:LOC docked to a mutated human βIV-tubulin (TUBB4 C239R)

Table 19:Table of the interactions between LOC and mutated human βIV-tubulin (TUBB4 C239R)

Ligand	Receptor	Interaction	Distance (A)	E (kcal/mol)
O4 1	N ASN 247 (A)	H-acceptor	3.29	-0.6

TUBB4 C239S

The S score obtained through MOE for this interaction is of S=-10.7526684, the geometry of the interaction is shown in Figure 27 and the type of interaction with the associated distance and energy are represented in Table 20.

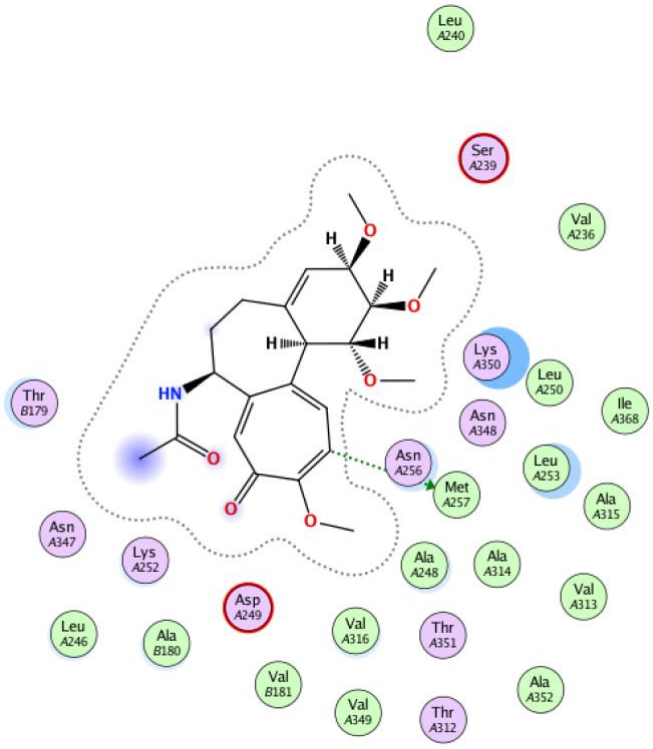

Figure 27:LOC docked to a mutated human βIV-tubulin (TUBB4 C239S)

Table 20:Table of the interactions between LOC and mutated human βIV-tubulin (TUBB4 C239S)

Ligand	Receptor	Interaction	Distance (A)	E (kcal/mol)
C19 49	SD MET 257 (A)	H-donor	3.79	-0.6

3.1.3 S score values

The S score values in Figure 28 should be intended a c a comparative measure of interaction affinity rather than being interpreted strictly for its physical significance.

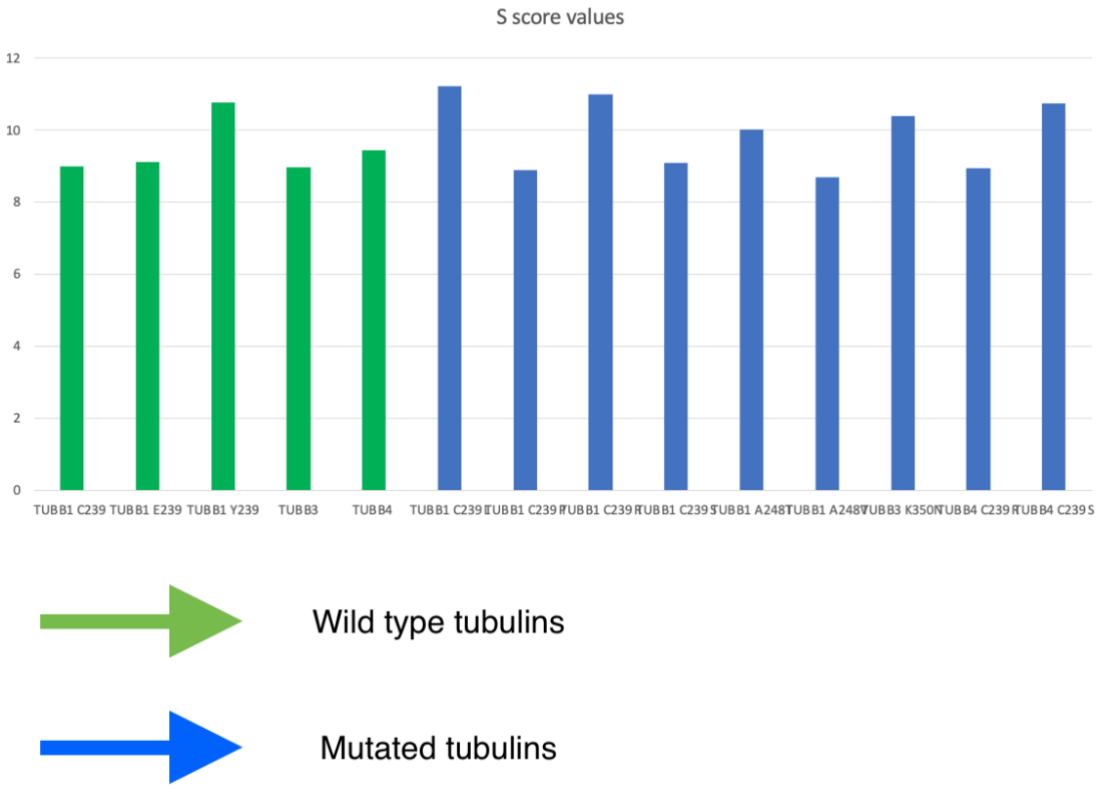

Figure 28:S score values in absolute value for mutated and not mutated tubulins

Discussion

The Alphafold2 predicted structures have been considered reliable. The tubulin β III by Alphafold2 superposed with the ".pdb" from RCSB database and the bovine tubulin compared with the mutated forms both shoved RMSD mean values below 2 Å, confirming the high quality of the models.

In evaluating the structural fidelity of Alphafold2's beta tubulin isotypes alongside human beta tubulin structures obtained through crystallography, an average RMSD value of approximately 1.07 Å was computed. This value, coupled with a remarkable Z score of -9.14, collectively furnishes robust evidence supporting the high caliber of the protein models.

Furthermore, the juxtaposition of the beta tubulin isotypes derived from Alphafold2 and bovine tissue's beta tubulin, as guided by experimental data, resulted in a remarkably low RMSD average mean value of 0.571 Å. Notably, this disparity falls well below the 2 Å threshold. This outcome definitively validates the decision to utilize the geometric characteristics of the colchicine binding site from bovine microtubules as a foundational template for constructing human heterodimers, leveraging the Alphafold2-derived tubulin.

The robust alignment observed between the Alphafold2 generated models and the corresponding animal tissue structures not only underscores the excellence of the models, but also emphasizes the potential suitability of animal tissue as a viable template for in vitro analyses.

To measure the affinity of the bond of colchicine in the colchicine binding site, the S score has been used. The S core in absolute value obtained through the docking simulations of the mutated and not mutated heterodimers are presented in Figure 28.

Comparing the S score values its notable that all the S score values are very high in absolute value, in rage between S=-11,23 (TUBB1 C239) and S=-8,70 (TUBB1 A248V). The high value absolute value of the S score represent the high affinity of colchicine for the binding site both in presence and without mutated beta tubulins.

It’s possible to notice that the value of the S score of the wild type tubulins is very close between each isomer, with an arithmetic mean value of 9,46 and a maximum value of 10.77 for TUBB1 Y239 and minimum value of 8.97 for TUBB3 in absolute value.

The value of the S score in the mutated forms analyzed shifts between S=- 11,23 (TUBB1 C239L) and S=-8,70 (TUBB1 A248V), with a mean absolute value of S=9,89. This result suggests two main factors. First, the values between the mutated and not mutated heterodimers aren’t significantly different, indicating that probably the affinity of colchicine isn’t influenced by the mutations.

One-Way ANOVA (Analysis of Variance)[8] test has been used to compare the S scores of two or more different groups of tubules. ANOVA is a statistical test used to analyze whether there are statistically significant differences among the means of three or more independent (unrelated) groups. In this case, each group is representing a different set of tubulins, the mutated and the wild type tubulins.[35]

The analysis yielded an F-ratio value of 0.99082. The associated p-value, calculated at 0.339192, indicates that the results are not statistically significant at the conventional significance level of $p < 0.05$. Consequently, there is insufficient evidence to reject the null hypothesis, suggesting that there are no statistically significant differences among the groups based on the S scores.

In second place, if the colchicine's affinity is influenced by the mutations, it's influenced by incrementing even if slightly the affinity, which is a good aspect in the vision of an antimitotic drug, that must be specific even for mutated tubulins.

The docking simulation confirmed the position of the experimental docking pocket. The interaction with the ligand is in every simulation an H-bond, which confirms the data present in literature. The interaction evolves always the 239th residue (TUBB1 E239 wild type, TUBB1 C239R, TUBB1 C239S, TUBB3 K350N), as confirmed by literature or/and the MET 257 residue (TUBB4 C239S, TUBB1 C239 wild type, TUBB1 E239 wild type, TUBB1 Y239 wild type, TUBB3 wild type, TUBB4 wild type, TUBB1 C239L, TUBB1 C239P, TUBB1 C239R, TUBB1 A248T, TUBB1 A248V, TUBB3 K350N, TUBB4 C239R), that is also part of the binding pocket. The H-bond on the MET 239 residue is present in every simulation, apart from the one involving TUBB1 C239S. The presence of the MET 257 H-bond is interesting, because not that evident in the analyzed literature, but not surprising because of the area of the bond.

It's interesting to compare the affinity of colchicine to tubulin, with the affinity of the most used anti-mitotic drug to treat cancer.

A similar procedure to obtain the entity of the affinity has been followed for some antimitotic drugs that are currently used to treat cancer. These drugs bind to tubulin in a different binding site that only involves beta tubulin.

[8] https://www.socscistatistics.com/tests/anova/default2.aspx

It has been calculated, through MOE, how the value of the S-score varies, to observe the energy differences between mutated tubulin and not mutated, with few chosen drugs: Paclitaxel (PTX) and Epothilone A.

From this comparison is evident how high is the affinity of colchicine for tubulin both in its mutated and not mutated form.

Table 21: S-score values in mutated and not mutated βI,III,IV tubulin docked with PTX

Beta1	no mut.	*L273P*	*C239L*	*C239Y*	*C239P*	-	-
S score	-7.87	-7.88	-7.48	-8.07	-7.81	-	-
Beta3	no mut.	*A231T*	*R282N*	*F270V*	*A275S*	*T274I*	Q292E
S score	-9.17	-8.54	-7.85	-8.88	-8.10	-7.80	-8.04
Beta4	no mut.	*S275A*	*Q292R*	*C239R*	-	-	-
S score	-7.54	-8.86	-8.30	-7.77	-	-	-

Table 22: S-score values in mutated and not mutated βI, III,IV tubulin docked with Ixabepilone

Beta1	No mut.	*L273P*	*C239L*	*C239Y*	*C239P*	-	-
S score	-6.87	-6.96	-7.01	-7.28	-6.87	-	-
Beta3	no mut.	*A231T*	*R282N*	*F270V*	*A275S*	*T274I*	Q292E
S score	-7.14	-7.15	-7.48	-7.75	-7.49	-7.40	-6.83
Beta4	no mut.	*S275A*	*Q292R*	*C239R*	-	-	-
S score	-7.64	-7.59	-7.16	-7.47	-	-	-

Conclusion

In conclusion, this study has successfully constructed a comprehensive computational model of the colchicine binding site within tubulin heterodimers, employing cutting-edge techniques such as AlphaFold2 and homology modeling guided by crystallographic data.

The comparison between the structures that have been built during this work and the animal structures resulting from crystallographic studies has determined both the reliability of the constructed structures and the good approximation in using animal tubules in the study of human drugs.

The focus has been on various forms of the heterodimer, particularly beta tubulin isotypes associated with cancer tissues, and rigorously validated the model against experimental data from animal studies. Through docking simulations, the impact of specific mutations within the colchicine binding site has been explored, shedding light on the variations in binding affinity.

In this study, the differential binding affinity of human tubulin isotypes beta 1, beta 3, beta4 and their main mutations towards colchicine have been investigated using molecular docking simulation and binding free energy calculations.

These findings not only enhance our understanding of how distinct beta tubulin mutations influence colchicine interactions but also hold great promise for the development of highly targeted colchicine-based cancer therapeutics. Ultimately, this research represents a significant advancement in the pursuit of more effective and specific treatments for cancer, with the hope for improved patient outcomes in the future.

It's important to notice that docking is a static approach and provides a snapshot of the predicted binding mode but doesn’t provide information on the dynamic behavior and interactions of the protein-ligand complex over time. A molecular dynamics simulation is then needed as a further approach.

Molecular dynamics is a simulation technique that allows researchers to study the movement and behavior of atoms and molecules in a system over a period of time. By applying Newton's laws of motion to each atom in the protein-ligand

complex, MD simulations can provide valuable information about the conformational changes, flexibility, and stability of the complex under different conditions.

Overall, molecular dynamics simulations would complement this molecular docking simulations by providing a more comprehensive understanding of the dynamic behavior of colchicine binding site of composed of wildtype and mutated tubulins, which is crucial for drug discovery, rational design, and understanding biological processes at the molecular level.

However, it is essential to acknowledge the inherent limitations of this computational approach. While our models have provided valuable insights into the colchicine binding site and its interactions with tubulin heterodimers, they are reliant on a variety of assumptions and simplifications. Homology modeling, although a powerful tool, is subject to inaccuracies when the target protein shares limited sequence identity with available templates. Additionally, the docking simulations represent a simplified representation of the dynamic binding process, which can be influenced by factors not considered in the models, such as solvent effects and conformational changes. Furthermore, the complexity of biological systems can sometimes elude even the most advanced computational techniques. Therefore, while this findings offer a promising direction for future research and drug development, they should be interpreted within the context of these inherent computational limitations, and further experimental validation will be crucial to confirm and refine our results.

Supplementary information

MATLAB SCRIPT

(https://docs.google.com/document/d/1NbOrVofNaNwbhKdhoYyhcQYHOqk-62ict0sHgNwn8NI/edit)

```
clc
clear
close

%scelta file template
[file1, path1] = uigetfile('*.fasta');
%scelta file contenente mutazioni
[file2, path2] = uigetfile('*.xlsx');

%Lettura file
[~,TUBB_template] = fastaread(['β-Tubulin Templates/',file1]);
TUBB_mut_table = readtable(['tabelle excel/',file2]);

L = length(TUBB_template); %lunghezza sequenza
N = height(TUBB_mut_table); %numero mutazioni
i = 1;

numbers_mut = TUBB_mut_table.Var2;
letters_mut = TUBB_mut_table.Var3;
letters_mut = char(letters_mut);

TUBB_true_matrix = TUBB_template;
for i = 1 : N-1
TUBB_true_matrix = [TUBB_true_matrix;TUBB_template];
end

TUBB_mut_true_matrix = TUBB_true_matrix;
for i = 1 : N
   TUBB_mut_true_matrix(i,numbers_mut(i)) = letters_mut(i);
end

for i = 1 : N
```

```
    data(i).Sequence = TUBB_mut_true_matrix(i,:);
    data(i).Header = [num2str(i) 'sequence'];
end

fastawrite('my_sequences.fasta', data)
```

List Of Figures

Figure 1- mechanism of action of stabilizer and destabiliser agents on MTs [6] 11
Figure 2: Colchicine's structure[9] 15
Figure 3: (a) Crystal structure of ab-tubulin heterodimers showing the binding sites of colchicine. (b) Interactions of colchicine with the colchicine-binding site of tubulin.[13] 16
Figure 4: human Tubulin alpha-1B from the Protein Data Bank [17] 18
Figure 5: 3D representation of the 5 simulated models of the tubulin b III by Alphafold2 superposed with the ".pdb" human tubulin from RSCB in green, from two different points of view 25
Figure 6: Z score value of wild-type human TUBB1 obtained with Alphafold2 is displayed in a plot. In this plot, structures from different sources (x-ray, NMR) are distinguished by different colours. 27
Figure 7: This plot shows local model quality by plotting energies as a function of amino acid sequence position i. In general, positive values correspond to problematic or erroneous parts of the input structure. 27
Figure 8: Bovine tubulin from RCSB [28] docked with colchicine. 29
Figure 9: RMSD between bovine beta tubulin (402B.B) and human mutated beta tubulin obtained through Alphafold2. The RMSD value associated to specific residues doesn't present peaks. 29
Figure 10: A) The RMSD of wild-type form of human tubulin TUBB1 E239, C239, Y239 and bovine tubulin (402B.B) is of 0.788 Å, B) between wild-type humanTUBB3 and bovine tubulin the value of RMSD is of 1.069 Å and C) the value of RMSD between wild-type human TUBB4 and bovine tubulin is of 1.113 Å. The RMSD shows some peak in correspondence on the residues that differ. 30
Figure 11: 3D structure of the obtained heterodimer composed by a beta tubulin structure from Alfafold2 and an alpha tubulin from RSCB. 33
Figure 12:legend for all following interactions of the ligand with the receptor from MOE 34
Figure 13:bovine tubulin heterodimer obtained through crystallography, in its interaction with colchicine. 35
Figure 14: LOC docked to human bI-tubulin (TUBB1 C239) 37
Figure 15:LOC docked to human bI-tubulin (TUBB1 E239) 38
Figure 16:LOC docked to human bI-tubulin (TUBB1 Y239) 39
Figure 17:LOC docked to human bIII-tubulin (TUBB3) 40
Figure 18:LOC docked to human bIV-tubulin (TUBB4) 41
Figure 19: LOC docked to a mutated human bI-tubulin (TUBB1 C239L) 42
Figure 20:LOC docked to a mutated human bI-tubulin (TUBB1 C239P) 43
Figure 21: LOC docked to a mutated human bI-tubulin (TUBB1 C239R) 44
Figure 22:LOC docked to a mutated human bI-tubulin (TUBB1 C239S) 45
Figure 23:LOC docked to a mutated human bI-tubulin (TUBB1 C248T) 46
Figure 24:LOC docked to a mutated human bI-tubulin (TUBB1 C248V) 47
Figure 25: LOC docked to a mutated human bIII-tubulin (TUBB3 K350N) 48
Figure 26:LOC docked to a mutated human bIV-tubulin (TUBB4 C239R) 49
Figure 27:LOC docked to a mutated human bIV-tubulin (TUBB4 C239S) 50
Figure 28:S score values in absolute value for mutated and not mutated tubulins 51

List Of Tables

Table 1: Principal Alteration of tubulin isotype [7].....12
Table 2:the table has been made with mutations of b-Tubulin. Mutations A231T, L240I, F270V, T274I, R282N, Q292E, R306C, K350N of bIII tubulin are from [6]. All other mutations come from the Tubulin Mutation Database (TMD). 19
Table 3: table shows b III-tubulin mutations for different animal species and human b- tubulin mutations. 20
Table 4: the table shows mutations of b-Tubulin, present in the colchicine binding site.....21
Table 5: Table of the average RMSD between the structures pictured in figure4, 5IJ0.B is the .pdb human tubulin from RSCB. The first five numbers are related to the five structures of human TUBB3 generated by Alphafold2. 26
Table 6: Table of the interactions between LOC and non-mutated crystallography bovine tubulin heterodimer.....34
Table 7: Table of the interactions between LOC and wild type human bI-tubulin (TUBB1 C239) 38
Table 8: Table of the interactions between LOC and wild type human bI-tubulin (TUBB1 E239).....38
Table 9: Table of the interactions between LOC and wild type human bI-tubulin (TUBB1 Y239).....39
Table 10: Table of the interactions between LOC and wild type human bIII-tubulin (TUBB3) 40
Table 11:Table of the interactions between LOC and wild type human bIV-tubulin (TUBB4) 41
Table 12:Table of the interactions between LOC and mutated human bI-tubulin (TUBB1 C239L) 42
Table 13:Table of the interactions between LOC and mutated human bI-tubulin (TUBB1 C239P) 43
Table 14:Table of the interactions between LOC and mutated human bI-tubulin (TUBB1 C239R) 44
Table 15:Table of the interactions between LOC and mutated human bI-tubulin (TUBB1 C239S) 45
Table 16:Table of the interactions between LOC and mutated human bI-tubulin (TUBB1 C248T) 46
Table 17:Table of the interactions between LOC and mutated human bI-tubulin (TUBB1 C248V) 47
Table 18: Table of the interactions between LOC and mutated human bIII-tubulin (TUBB3 K350N) 48
Table 19:Table of the interactions between LOC and mutated human bIV-tubulin (TUBB4 C239R) 49
Table 20:Table of the interactions between LOC and mutated human bIV-tubulin (TUBB4 C239S) 50
Table 21: S-score values in mutated and not mutated bI,III,IV tubulin docked with PTX 54
Table 22: S-score values in mutated and not mutated bI,III,IV tubulin docked with Ixabepilone 54

References

1. Jumper, J.; Evans, R.; Pritzel, A.; Green, T.; Figurnov, M.; Ronneberger, O.; Tunyasuvunakool, K.; Bates, R.; Žídek, A.; Potapenko, A.; et al. Highly Accurate Protein Structure Prediction with AlphaFold. *Nature* **2021**, *596*, 583–589, doi:10.1038/s41586-021-03819-2.
2. Moore, M.A.; Goodman, R.A. Physician Training in Cancer Prevention and Control: A Population Health Imperative. *Am J Prev Med* **2018**, *54*, 444–448, doi:10.1016/j.amepre.2017.10.020.
3. Risinger, A.L.; Giles, F.J.; Mooberry, S.L. Microtubule Dynamics as a Target in Oncology. *Cancer Treat Rev* **2009**, *35*, 255–261, doi:10.1016/j.ctrv.2008.11.001.
4. Risinger, A.L.; Giles, F.J.; Mooberry, S.L. Microtubule Dynamics as a Target in Oncology. *Cancer Treat Rev* 2009, *35*, 255–261.
5. Kavallaris, M. Microtubules and Resistance to Tubulin-Binding Agents. *Nat Rev Cancer* 2010, *10*, 194–204.
6. Huzil, J.T.; Chen, K.; Kurgan, L.; Tuszynski, J.A. *The Roles of β-Tubulin Mutations and Isotype Expression in Acquired Drug Resistance*; 2007;
7. Van Vuuren, R.J.; Visagie, M.H.; Theron, A.E.; Joubert, A.M. Antimitotic Drugs in the Treatment of Cancer. *Cancer Chemother Pharmacol* 2015, *76*, 1101–1112.
8. Kumbhar, B.V.; Borogaon, A.; Panda, D.; Kunwar, A. Exploring the Origin of Differential Binding Affinities of Human Tubulin Isotypes AβII, AβIII and AβIV for DAMA-Colchicine Using Homology Modelling, Molecular Docking and Molecular Dynamics Simulations. *PLoS One* **2016**, *11*, doi:10.1371/journal.pone.0156048.
9. Slobodnick, A.; Shah, B.; Pillinger, M.H.; Krasnokutsky, S. Colchicine: Old and New. *American Journal of Medicine* 2015, *128*, 461–470.
10. Sivakumar, G. *Send Orders of Reprints at Reprints@benthamscience.Net Colchicine Semisynthetics: Chemotherapeutics for Cancer?*; 2013; Vol. 20;.
11. Pallante, L.; Rocca, A.; Klejborowska, G.; Huczynski, A.; Grasso, G.; Tuszynski, J.A.; Deriu, M.A. In Silico Investigations of the Mode of Action of Novel Colchicine Derivatives Targeting β-Tubulin Isotypes: A Search for a Selective and Specific β-III Tubulin Ligand. *Front Chem* **2020**, *8*, doi:10.3389/fchem.2020.00108.
12. Lu, Y.; Chen, J.; Xiao, M.; Li, W.; Miller, D.D. An Overview of Tubulin Inhibitors That Interact with the Colchicine Binding Site. *Pharm Res* 2012, *29*, 2943–2971.
13. Kumar, A.; Sharma, P.R.; Mondhe, D.M. Potential Anticancer Role of Colchicine-Based Derivatives: An Overview. *Anticancer Drugs* 2016, *28*, 250–262.
14. Ravelli, R.B.G.; Gigant, B.; Curmi, P.A.; Jourdain, I.; Lachkar, S.; Sobel, A.; Knossow, M. Insight into Tubulin Regulation from a Complex with Colchicine and a Stathmin-like Domain. *Nature* **2004**, *428*, 198–202, doi:10.1038/nature02393.
15. Bhattacharyya, B.; Panda, D.; Gupta, S.; Banerjee, M. Anti-Mitotic Activity of Colchicine and the Structural Basis for Its Interaction with Tubulin. *Med Res Rev* 2008, *28*, 155–183.
16. Valasek, L.S. et al. Functional Characterization of Human Alpha-Tubulin Genes by Complementation in Yeast Mutants. *Journal of Cell Science* **1998**, *111*, 3339–3352.

17. Ti, S.-C.; Alushin, G.M.; Kapoor, T.M. Human β-Tubulin Isotypes Can Regulate Microtubule Protofilament Number and Stability. *Dev Cell* **2018**, *47*, 175-190.e5, doi:10.1016/j.devcel.2018.08.014.
18. Yang, J.; Li, Y.; Yan, W.; Li, W.; Qiu, Q.; Ye, H.; Chen, L. Covalent Modification of Cys-239 in β-Tubulin by Small Molecules as a Strategy to Promote Tubulin Heterodimer Degradation. *Journal of Biological Chemistry* **2019**, *294*, 8161–8170, doi:10.1074/jbc.RA118.006325.
19. Yang, J.; Li, Y.; Yan, W.; Li, W.; Qiu, Q.; Ye, H.; Chen, L. Covalent Modification of Cys-239 in β-Tubulin by Small Molecules as a Strategy to Promote Tubulin Heterodimer Degradation. *Journal of Biological Chemistry* **2019**, *294*, 8161–8170, doi:10.1074/jbc.RA118.006325.
20. Wang, W.; Zhang, H.; Wang, X.; Patterson, J.; Winter, P.; Graham, K.; Ghosh, S.; Lee, J.C.; Katsetos, C.D.; Mackey, J.R.; et al. Novel Mutations Involving BI-, BIIA-, or BIVB-Tubulin Isotypes with Functional Resemblance to BIII-Tubulin in Breast Cancer. *Protoplasma* **2017**, *254*, 1163–1173, doi:10.1007/s00709-016-1060-1.
21. Spasevska, I.; Ayoub, A.T.; Winter, P.; Preto, J.; Wong, G.K.S.; Dumontet, C.; Tuszynski, J.A. Modeling the Colchicum Autumnale Tubulin and a Comparison of Its Interaction with Colchicine to Human Tubulin. *Int J Mol Sci* **2017**, *18*, doi:10.3390/ijms18081676.
22. Tickle, I.J. Experimental Determination of Optimal Root-Mean-Square Deviations of Macromolecular Bond Lengths and Angles from Their Restrained Ideal Values. *Acta Crystallogr D Biol Crystallogr* **2007**, *63*, 1274–1281, doi:10.1107/S0907444907050196.
23. Michino, M.; Abola, E.; Brooks, C.L.; Dixon, J.S.; Moult, J.; Stevens, R.C. Community-Wide Assessment of GPCR Structure Modelling and Ligand Docking: GPCR Dock 2008. *Nat Rev Drug Discov* **2009**, *8*, 455–463, doi:10.1038/nrd2877.
24. Ti, S.-C.; Pamula, M.C.; Howes, S.C.; Duellberg, C.; Cade, N.I.; Kleiner, R.E.; Forth, S.; Surrey, T.; Nogales, E.; Kapoor, T.M. Mutations in Human Tubulin Proximal to the Kinesin-Binding Site Alter Dynamic Instability at Microtubule Plus- and Minus-Ends. *Dev Cell* **2016**, *37*, 72–84, doi:10.1016/j.devcel.2016.03.003.
25. Akbari, V.; Moghim, S.; Reza Mofid, M. Comparison of Epothilone and Taxol Binding in Yeast Tubulin Using Molecular Modeling. *Avicenna J Med Biotechnol* **2011**, *3*, 167–175.
26. Wiederstein, M.; Sippl, M.J. ProSA-Web: Interactive Web Service for the Recognition of Errors in Three-Dimensional Structures of Proteins. *Nucleic Acids Res* **2007**, *35*, W407–W410, doi:10.1093/nar/gkm290.
27. Sippl, M.J. Recognition of Errors in Three-Dimensional Structures of Proteins. *Proteins: Structure, Function, and Genetics* **1993**, *17*, 355–362, doi:10.1002/prot.340170404.
28. Prota, A.E.; Danel, F.; Bachmann, F.; Bargsten, K.; Buey, R.M.; Pohlmann, J.; Reinelt, S.; Lane, H.; Steinmetz, M.O. The Novel Microtubule-Destabilizing Drug BAL27862 Binds to the Colchicine Site of Tubulin with Distinct Effects on Microtubule Organization. *J Mol Biol* **2014**, *426*, 1848–1860, doi:10.1016/j.jmb.2014.02.005.
29. Janakiraman, V.; Sudhan, M.; Alzahrani, K.J.; Alshammeri, S.; Ahmed, S.S.S.J.; Patil, S. Dynamics of TUBB Protein with Five Majorly Occurring Natural Variants: A Risk of Cortical Dysplasia. *J Mol Model* **2023**, *29*, doi:10.1007/s00894-023-05506-7.
30. Prota, A.E.; Danel, F.; Bachmann, F.; Bargsten, K.; Buey, R.M.; Pohlmann, J.; Reinelt, S.; Lane, H.; Steinmetz, M.O. The Novel Microtubule-Destabilizing Drug BAL27862 Binds to the Colchicine Site of Tubulin with Distinct Effects on Microtubule Organization. *J Mol Biol* **2014**, *426*, 1848–1860, doi:10.1016/j.jmb.2014.02.005.

31. Kumbhar, B.V.; Borogaon, A.; Panda, D.; Kunwar, A. Exploring the Origin of Differential Binding Affinities of Human Tubulin Isotypes AβII, AβIII and AβIV for DAMA-Colchicine Using Homology Modelling, Molecular Docking and Molecular Dynamics Simulations. *PLoS One* **2016**, *11*, doi:10.1371/journal.pone.0156048.
32. Paal, K.; Shkarupin, A.; Beckford, L. Paclitaxel Binding to Human Serum Albumin-Automated Docking Studies. *Bioorg Med Chem* **2007**, *15*, 1323–1329, doi:10.1016/j.bmc.2006.11.012.
33. Li, J.; Fu, A.; Zhang, L. An Overview of Scoring Functions Used for Protein–Ligand Interactions in Molecular Docking. *Interdiscip Sci* **2019**, *11*, 320–328, doi:10.1007/s12539-019-00327-w.
34. Bueno, O.; Estévez Gallego, J.; Martins, S.; Prota, A.E.; Gago, F.; Gómez-SanJuan, A.; Camarasa, M.-J.; Barasoain, I.; Steinmetz, M.O.; Díaz, J.F.; et al. High-Affinity Ligands of the Colchicine Domain in Tubulin Based on a Structure-Guided Design. *Sci Rep* **2018**, *8*, 4242, doi:10.1038/s41598-018-22382-x.
35. Kim, T.K. Understanding One-Way ANOVA Using Conceptual Figures. *Korean J Anesthesiol* **2017**, *70*, 22, doi:10.4097/kjae.2017.70.1.22.